Article

Neuron

Encoding of Discriminative Fear Memory by Input-Specific LTP in the Amygdala

Highlights

- LTP is not induced globally in ACx/MGN-LA pathways in discriminative fear learning
- LTP is induced in CS+, but not CS–, pathways to LA in discriminative fear learning
- Synapses in CS+ pathways to LA remain potentiated after fear extinction
- Depotentiation of CS+, but not CS–, pathways to LA prevents the recall of fear memory

Authors

Woong Bin Kim, Jun-Hyeong Cho

Correspondence

juncho@ucr.edu

In Brief

Kim and Cho demonstrate that the formation of fear memory associated with a specific auditory cue requires selective synaptic strengthening in functionally defined neural pathways that convey the auditory signals to the amygdala.

Kim & Cho, 2017, Neuron *95*, 1129–1146
August 30, 2017
http://dx.doi.org/10.1016/j.neuron.2017.08.004

CellPress

Neuron
Article

Encoding of Discriminative Fear Memory by Input-Specific LTP in the Amygdala

Woong Bin Kim[1] and Jun-Hyeong Cho[1,2,*]
[1]Department of Molecular, Cell, and Systems Biology, University of California, Riverside, Riverside, CA 92521, USA
[2]Lead Contact
*Correspondence: juncho@ucr.edu
http://dx.doi.org/10.1016/j.neuron.2017.08.004

SUMMARY

In auditory fear conditioning, experimental subjects learn to associate an auditory conditioned stimulus (CS) with an aversive unconditioned stimulus. With sufficient training, animals fear conditioned to an auditory CS show fear response to the CS, but not to irrelevant auditory stimuli. Although long-term potentiation (LTP) in the lateral amygdala (LA) plays an essential role in auditory fear conditioning, it is unknown whether LTP is induced selectively in the neural pathways conveying specific CS information to the LA in discriminative fear learning. Here, we show that postsynaptically expressed LTP is induced selectively in the CS-specific auditory pathways to the LA in a mouse model of auditory discriminative fear conditioning. Moreover, optogenetically induced depotentiation of the CS-specific auditory pathways to the LA suppressed conditioned fear responses to the CS. Our results suggest that input-specific LTP in the LA contributes to fear memory specificity, enabling adaptive fear responses only to the relevant sensory cue.

INTRODUCTION

To survive in a dynamic environment, animals develop fear responses to dangerous situations. For these adaptive fear responses to be developed, the brain must discriminate between different sensory cues and associate only relevant stimuli with aversive events. In auditory fear conditioning, an experimental model of fear learning, experimental subjects learn to associate an emotionally neutral auditory conditioned stimulus (CS; e.g., a tone) with an aversive unconditioned stimulus (US; e.g., electric foot shock), displaying conditioned fear responses (e.g., freezing behavior) to the neutral CS (LeDoux, 2000; Maren, 2001; Tovote et al., 2015). With sufficient training, animals fear conditioned to an auditory stimulus show fear responses to the same stimulus, but not to irrelevant auditory stimuli. It is poorly understood at the neuronal and synaptic levels how animals discriminate between auditory stimuli to show fear responses selectively to the relevant stimulus.

Long-term potentiation (LTP) in the amygdala plays an essential role in the formation of conditioned fear memory (Cho et al., 2011; McKernan and Shinnick-Gallagher, 1997; Nabavi et al., 2014; Rogan et al., 1997; Rumpel et al., 2005; Tsvetkov et al., 2002). After fear conditioning, synaptic strength is enhanced in the auditory CS pathways to the lateral nucleus of the amygdala (LA), such that presentation of the CS alone is sufficient to activate the amygdala and its downstream brain areas (Tovote et al., 2016), resulting in fear responses to the CS. A specific auditory CS activates only a subset of neurons in the auditory cortex (ACx) and thalamus (medial geniculate nucleus, MGN), which convey CS information to the amygdala for the CS-US association. Thus, LTP may be induced selectively in neural circuits conveying specific CS signals to the amygdala for encoding fear memory for the CS. After fear conditioning with the auditory CS+, auditory-evoked single-unit activity and local field potential in the LA are enhanced more robustly to the CS+ (a relevant stimulus) than to the CS– (an irrelevant stimulus), suggesting a selective increase in the responsiveness of LA neurons to the CS+ (Collins and Paré, 2000; Ghosh and Chattarji, 2015; Goosens et al., 2003). However, it has not been determined whether LTP is induced selectively in neural pathways conveying specific CS information to the amygdala in discriminative fear learning. If LTP in the CS-specific pathways confers fear memory specificity, fear memory for the CS could be erased selectively by depotentiation, reversing the input-specific LTP. However, it has not been examined whether depotentiation in the CS-specific pathways to the amygdala suppresses fear memory for the CS.

To determine the synaptic mechanisms of how discriminative fear memory for a specific CS is encoded in the amygdala, we tested our hypothesis that specific fear memory is encoded by selective LTP in neural pathways defined by presynaptic inputs conveying specific CS information to the amygdala. Using a combined approach of neural activity-dependent behavioral labeling (Guenthner et al., 2013), optogenetic stimulations (Yizhar et al., 2011), and electrophysiological recordings (Cho et al., 2013), we found that postsynaptically expressed LTP was induced selectively in the CS-specific ACx/MGN-LA pathways after auditory discriminative fear conditioning in mice, whereas LTP was not detected in randomly selected ACx/MGN-LA pathways. Moreover, optogenetically induced depotentiation of the CS-specific ACx/MGN-LA pathways prevented the recall of fear memory for the auditory CS. Thus, input-specific LTP in the LA could contribute to fear memory specificity, enabling adaptive fear responses only to the relevant sensory cue.

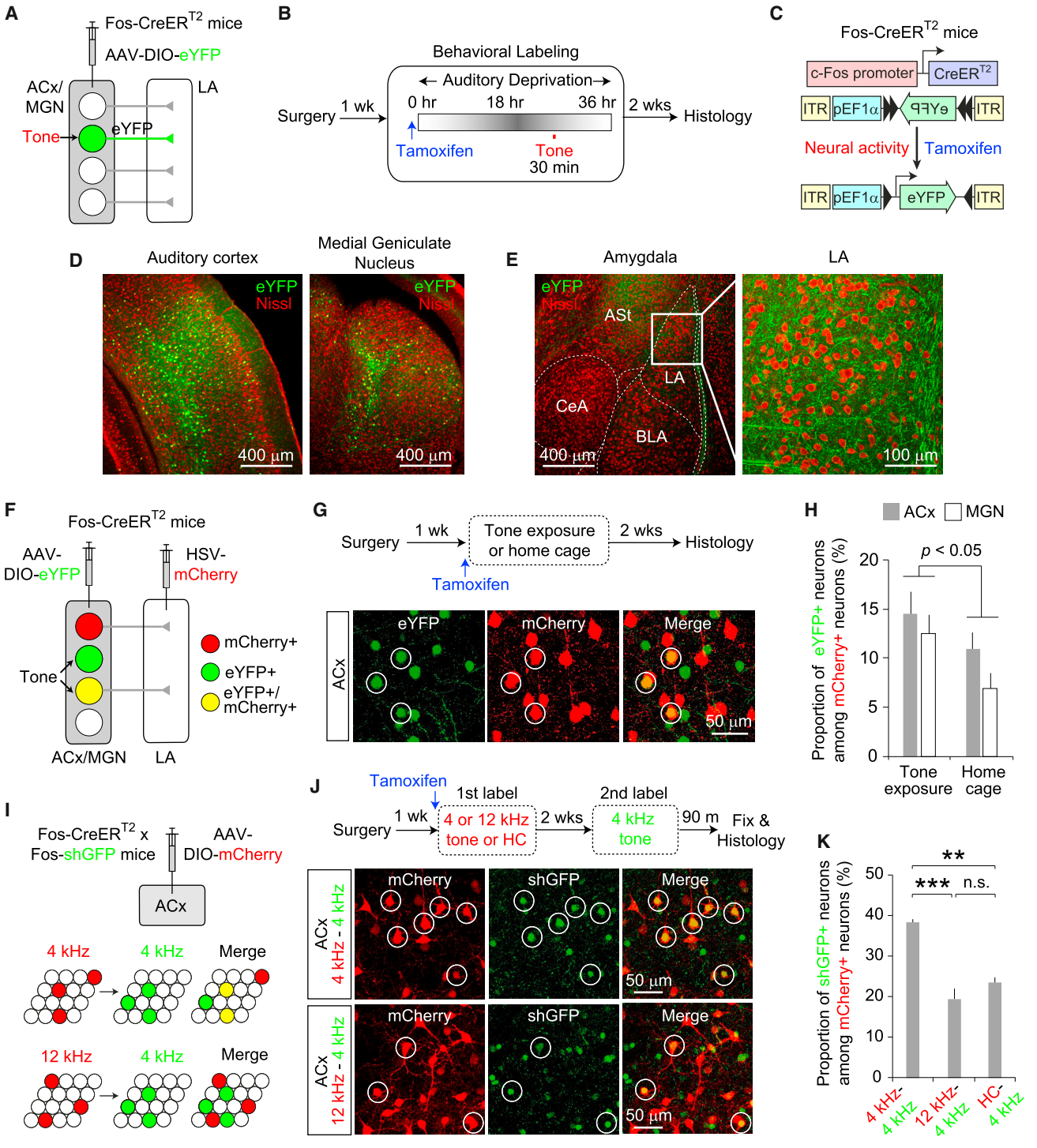

Figure 1. Behavioral Labeling of ACx/MGN Neurons Responding to a Specific Auditory Stimulus

(A) Experimental setup for (B)–(E). Tone-responding ACx/MGN neurons were labeled with eYFP (green).

(B) Behavioral labeling protocol. After surgery, the mice received a tamoxifen injection and were exposed to a 4 or 12 kHz tone for 30 min.

(C) A population of ACx/MGN neurons responding to the auditory stimulus expresses CreER^{T2} under the control of the c-Fos promoter, resulting in permanent eYFP expression.

(D) Microscopic images of coronal brain sections showing eYFP expression (green) in ACx and MGN. Red fluorescence is Nissl stain.

(E) Microscopic images of the amygdala and LA showing eYFP-labeled axons of behaviorally labeled ACx/MGN neurons. BLA and CeA, basolateral and central nuclei of the amygdala, respectively. ASt, amygdalo-striatal transition area.

(legend continued on next page)

RESULTS

Behavioral Labeling of ACx/MGN Neurons Responding to a Specific Auditory Stimulus

To examine synaptic changes in the auditory CS-specific pathways to the LA, we employed a behavioral labeling approach with Fos-CreER^{T2} knockin mice (Guenthner et al., 2013). We injected adeno-associated virus (AAV) encoding the eYFP gene in a double inverse open reading frame (DIO) (AAV-pEF1α-DIO-eYFP) into ACx and MGN in heterozygous Fos-CreER^{T2} mice (Figure 1A) and exposed them to a 4 or 12 kHz tone (5 s duration, 15 s interval) for 30 min after tamoxifen administration (Figures 1B and S1A). A population of ACx/MGN neurons responding to the tone expressed CreER^{T2} under the control of an activity-dependent endogenous c-Fos promoter, which then induced the recombination of the DIO in the presence of tamoxifen, resulting in permanent eYFP expression (Figure 1C). Two weeks after the behavioral labeling, eYFP expression was detected in a subset of ACx/MGN neurons (Figure 1D). Within the amygdala, eYFP-labeled projections were found predominantly in the LA (Figure 1E). Without tamoxifen injection before tone exposure, eYFP expression was detected in only a few neurons in ACx and MGN (Figure S1B).

Next, we quantified the proportion of behaviorally labeled neurons among ACx/MGN neurons projecting to the LA. We injected AAV-pEF1α-DIO-eYFP to ACx and MGN and retrograde herpes simplex virus (HSV) encoding the mCherry gene into the LA in Fos-CreER^{T2} mice (Figure 1F). After the behavioral labeling, tone-responding ACx/MGN neurons were labeled with eYFP, whereas LA-projecting neurons were labeled with mCherry (Figures 1G and S1C). Our behavioral labeling resulted in eYFP expression in 14.6% ± 2.3% and 12.5% ± 1.9% of ACx and MGN neurons projecting to the LA, respectively (mean ± SEM, 7 mice; Figure 1H). The proportion was significantly higher in tone-exposed mice compared with mice left in home cages under auditory deprivation (Figure 1H; Table S1), indicating that behaviorally labeled neurons included tone-responding ACx/MGN neurons.

To examine the specificity of our behavioral labeling method, we labeled ACx/MGN neurons with different fluorescent proteins during the first and second tone exposures. We injected AAV-pEF1α-DIO-mCherry into ACx and MGN in Fos-CreER^{T2} × Fos-shGFP mice, which express both CreER^{T2} and short half-life (2 hr) GFP (shGFP) under the control of the c-Fos promoter (Reijmers et al., 2007) (Figures 1I and S1D). After receiving tamoxifen, these mice were exposed to a 4 or 12 kHz tone or left in home cages (HCs) for mCherry expression in ACx and MGN (Figures 1J and S1E). Two weeks later, the mice were exposed to a 4 kHz tone for shGFP expression, and the brain tissues were fixed 90 min later. The proportion of double-labeled ACx/MGN neurons (mCherry+/shGFP+) among all mCherry+ neurons was significantly higher in mice exposed to the same tone (4 kHz-4 kHz tone) than in mice exposed to different tones (12 kHz-4 kHz tone) or in mice of the HC-4 kHz tone group (Figures 1J, 1K, S1E, and S1F; Table S1). These results indicate the specificity of our behavioral labeling approach.

LA Neuronal Ensemble Defined by Presynaptic ACx/MGN Inputs Conveying Specific Auditory Information

With our behavioral labeling approach, we examined how each LA neuron received ACx/MGN inputs conveying specific auditory information. We injected AAV-pEF1α-DIO-ChR2-eYFP into ACx and MGN in Fos-CreER^{T2} mice and exposed them to a 4 or 12 kHz tone after tamoxifen administration (Figures 2A and 2B). Three weeks later, tone-responding ACx/MGN neurons expressed ChR2-eYFP, and eYFP-labeled projections were found in the LA (Figure 2C). To induce synaptic responses in the tone-specific ACx/MGN-LA pathways, we applied blue light illumination to activate ChR2-expressing axons in the LA in brain slices and recorded postsynaptic responses in principal neurons of the LA using a whole-cell patch-clamp technique (Figures 2A, 2D, and 2E). Short pulses of photostimulation induced monosynaptic excitatory postsynaptic currents (EPSCs) at –80 mV in voltage-clamp mode, which were completely blocked by glutamate receptor antagonists, indicating that these EPSCs were mediated by glutamate ($p < 0.01$, paired t test; Figures 2D and S2A–S2D; Table S2). Both ACx and MGN axons labeled with different fluorescent proteins were detected in the LA, suggesting their role in conveying auditory information to the amygdala (Figures S2E–S2G). Independent photostimulations of either the tone-labeled ACx or MGN axons induced EPSCs in the same LA neurons, indicating that LA neurons received inputs from both ACx and MGN conveying specific auditory information (Figures S2H–S2K).

The peak amplitude of EPSCs recorded in the tone-specific ACx/MGN-LA pathways was proportional to the light power

(F) Experimental setup for (G) and (H). Tone-responding ACx/MGN neurons were labeled with eYFP (green), and LA-projecting neurons were labeled with mCherry (red).

(G) Top: after tamoxifen injection, mice were exposed to the 4 kHz tone as in (B) (tone exposure group), whereas mice in the control group were left in their home cages. Bottom: magnified images of ACx in the tone exposure group. Tone-responding neurons were labeled with eYFP (green), and LA-projecting neurons were labeled with mCherry (red). Neurons expressing both eYFP and mCherry are marked with white circles.

(H) Quantification of the proportion of behaviorally labeled neurons (eYFP+) among all LA-projecting ACx/MGN neurons (mCherry+). n = 6–7 mice per group.

(I) Top: experimental setup for (J) and (K). Bottom: ACx neurons responding to the 4 or 12 kHz tone were first labeled with mCherry (red). Mice were then exposed to the 4 kHz tone for shGFP expression (green).

(J) Top: after tamoxifen injection, mice in the 4 kHz-4 kHz tone group were exposed to the 4 kHz tone, and mice in the 12 kHz-4 kHz tone group were exposed to the 12 kHz tone, whereas mice in the HC-4 kHz tone group were left in home cages (HCs). Two weeks later, mice were exposed to the 4 kHz tone. Middle and bottom: representative images showing ACx neurons labeled with mCherry (red) and/or shGFP (green). ACx neurons activated during the first and second tone exposures expressed both mCherry and shGFP (white circles).

(K) Quantification of the proportion of shGFP+ neurons among all mCherry+ ACx neurons (n = 4 mice per group). $^{**}p < 0.01$, $^{***}p < 0.001$; n.s., non-significant. Error bars indicate SEM.

See also Figure S1.

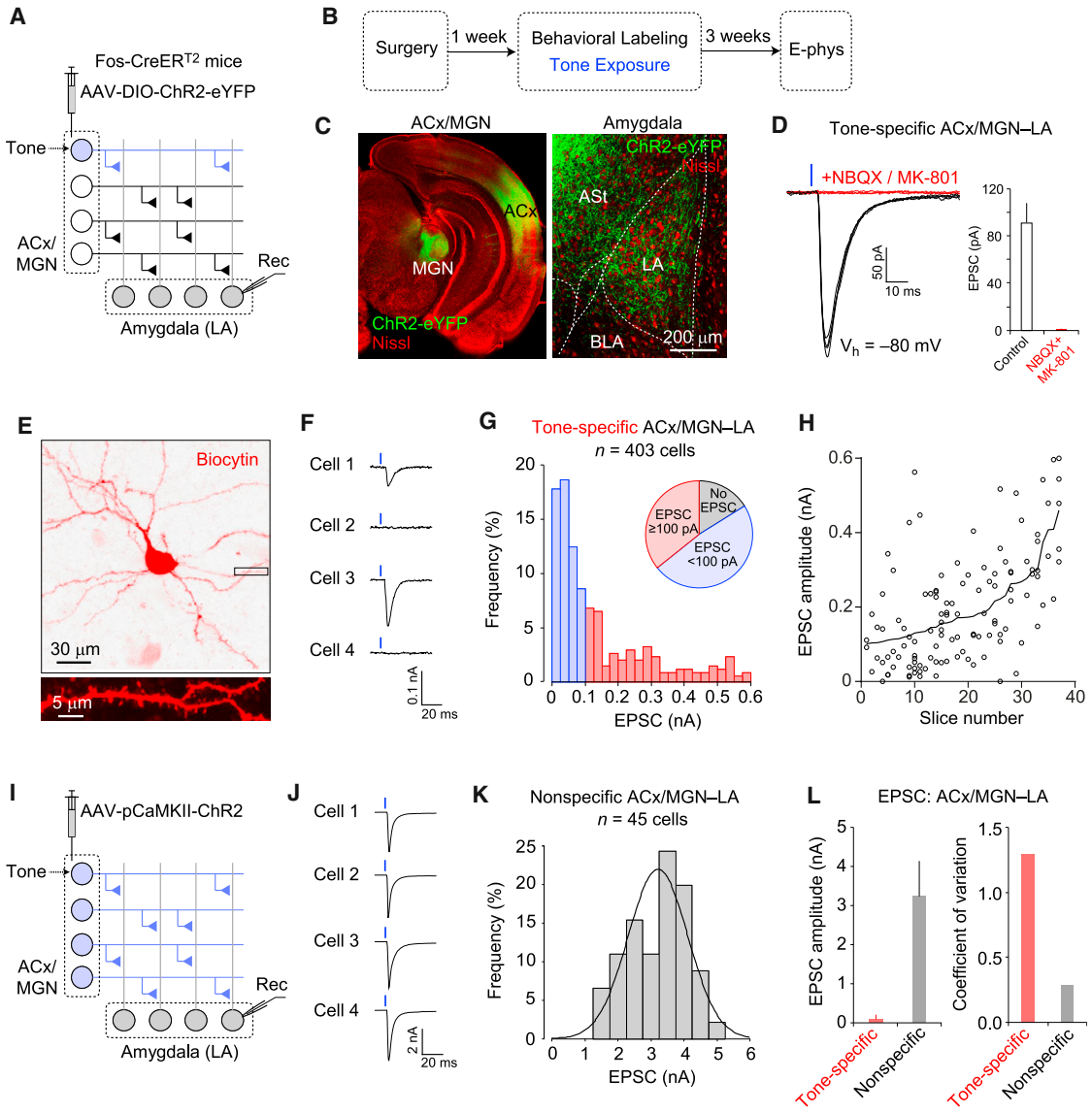

Figure 2. LA Neuronal Ensemble Defined by Presynaptic ACx/MGN Inputs Conveying Specific Auditory Information

(A) Experimental setup for (B)–(H) and a neural circuit diagram of tone-specific ACx/MGN-LA pathways. After behavioral labeling, tone-responding ACx/MGN neurons expressed ChR2-eYFP (blue). Local blue light illumination in the amygdala activated ChR2-expressing axons and induced postsynaptic responses in LA neurons (Rec). Horizontal lines indicate ACx/MGN axons projecting to the LA, and vertical lines indicate the dendrites of LA neurons.

(B) After tamoxifen injection, mice were exposed to the 4 or 12 kHz tone for behavioral labeling as in Figure 1B. Electrophysiological recordings (E-phys) were performed 3 weeks later.

(C) Microscopic images of the ACx/MGN and amygdala showing ChR2-eYFP-expressing projections (green). Red fluorescence is Nissl stain.

(D) Left: representative traces of excitatory postsynaptic currents (EPSCs) recorded in a principal neuron of the LA (black). EPSCs were induced by photostimulation (470 nm LED, 20.0 mW/mm^2, 1 ms duration, blue vertical bar) of ChR2-expressing ACx/MGN axons and recorded at –80 mV in voltage-clamp mode. EPSCs were inhibited completely by NBQX (10 μM) and MK-801 (10 μM) (red). Right: quantification of EPSC inhibition by NBQX and MK-801 (n = 7 cells). Error bars are SEM.

(E) Microscopic image of a principal neuron of the LA loaded with biocytin during whole-cell patch-clamp recording and labeled with streptavidin-Alexa 568 (red, top). A section of dendrites of the labeled neuron is shown below in a higher magnification (bottom).

(F) EPSCs recorded in four LA neurons in a brain slice. EPSCs were induced by photostimulation of the same intensity and recorded as in (D).

(G) Histogram showing the distribution of the peak amplitude of EPSCs induced and recorded as in (D).

(H) Scatterplot of the peak amplitude of EPSCs recorded in multiple LA neurons in each brain slice. Open circles indicate EPSC amplitude in individual LA neurons. The average amplitude of EPSC recorded in LA neurons in each brain slice (a black curve) was used to sort data along the x axis in increasing order.

(I) Experimental setup for (J) and (K). AAV-pCaMKIIα-ChR2-eYFP was injected into ACx and MGN to induce global expression of ChR2.

(J) EPSCs induced by nonselective photostimulation of the ACx/MGN-LA pathways and recorded at –65 mV in four LA neurons in a brain slice.

(legend continued on next page)

density (Figure S2L). EPSCs recorded in different LA neurons in the same brain slice were heterogeneous (Figures 2F–2H), and the distribution of EPSC amplitude was highly skewed (Figure 2G). Moreover, robust EPSCs were detected only in a subset of LA neurons, whereas 64.3% of the LA neurons displayed either no synaptic responses or EPSCs with modest amplitude (<100 pA; Figure 2G). However, when ACx/MGN neurons globally expressed ChR2 and their axons were randomly stimulated as in Figure 2I, the EPSC amplitude was much larger but normally distributed ($p = 0.13$, Anderson-Darling normality test), with less variability than EPSCs in tone-specific ACx/MGN-LA pathways (Figures 2J–2L, S2L, and S2M). Together, these results suggest that a subset of LA neurons preferentially receive presynaptic ACx/MGN inputs relaying specific auditory information (Figures S2N–S2Q) (Gründemann and Lüthi, 2015).

Postsynaptically Expressed LTP Was Induced in the CS+ Pathways to the LA in Auditory Discriminative Fear Conditioning

To investigate the synaptic mechanisms of fear memory specificity, we developed a behavioral protocol for discriminative auditory fear conditioning, in which mice were trained to show conditioned fear response (e.g., freezing behavior) selectively to an auditory cue, CS+ (Figures 3A and S3A–S3C). After single-trial fear conditioning, in which CS+ (4 or 12 kHz tone, counterbalanced) was presented paired with the US (foot shock, 0.5 mA, 2 s duration), mice displayed non-discriminative fear to both the CS+ and CS–, which was not paired with the US (day 2 in Figures 3B and 3C). After multiple-trial fear conditioning, however, mice showed fear selectively to the CS+ (day 6 in Figures 3B and 3C) with better discrimination between the CS+ and CS– ($p < 0.001$, paired t test; Figure 3C).

We next examined how synaptic efficacy changes in the ACx/MGN inputs conveying CS+ information to the LA in discriminative fear conditioning. As we were unable to predict whether LTP would be induced in both the ACx-LA and MGN-LA pathways or would be confined to either of these two pathways in discriminative fear conditioning, we first examined LTP in these pathways altogether. We injected AAV-pEF1α-DIO-ChR2-eYFP into both ACx and MGN in Fos-CreER^{T2} mice to induce ChR2 expression in ACx/MGN neurons responding to the CS+ (Figures 3D–3F). After behavioral labeling, mice in the fear conditioning (FC) group were trained for discriminative fear learning (Figures 3A and 3E) and displayed discriminative fear to the CS+ (Figures 3G and S3D). Mice in the no shock (NS) control group received the CS+ and CS– as in the FC group but without the US and did not show fear responses to either the CS+ or CS– (Figure 3G). In brain slices from these mice, we recorded EPSCs in principal neurons in the LA, which were differentiated from GABAergic interneurons based on their passive membrane properties (Figures S4A–S4D). Photostimulations of ChR2-expressing axons in the LA induced EPSCs, which reflect postsynaptic responses in the CS+ pathways to the LA (Figures 3D and 3H). The induction of LTP and long-term depression (LTD) in the ACx/MGN-LA pathways in brain slices was accompanied by changes in the AMPA/NMDA EPSC ratio (Figures S4E–S4L), which correlated with the magnitude of LTP and LTD (Figure S4M; correlation coefficient $r = 0.89$; $p < 0.001$), suggesting that the changes in the AMPA/NMDA ratio reliably reflect long-term synaptic plasticity in the ACx/MGN-LA pathways (Kauer et al., 1988; Muller et al., 1988). Thus, to detect changes in synaptic strength in the CS+ pathways by postsynaptic expression mechanisms in discriminative fear learning, we compared the AMPA/NMDA ratio between the FC and NS groups. We recorded both AMPA receptor (AMPAR)- and NMDA receptor (NMDAR)-mediated EPSCs in the same LA neurons and calculated the AMPA/NMDA ratio (Figure 3H). The AMPA/NMDA ratio was significantly higher in the FC group than in the NS group (Figures 3H–3J; main effect of groups, $p < 0.001$; main effect of tone frequency, $p = 0.90$; groups × tone frequency interaction, $p = 0.49$; two-way ANOVA), whereas the passive membrane properties of recorded LA neurons were not different between groups (Table S3). In 19.4% of all the LA neurons in the FC group, the AMPA/NMDA ratio was larger than the average AMPA/NMDA ratio in the NS group by more than two SDs (Figure 3I), suggesting that these LA neurons underwent LTP in the CS+ pathways (Rumpel et al., 2005).

Enhanced synaptic efficacy in the CS+ pathways was detected only when the CS+ was presented temporally paired with the US on the training day ($p < 0.05$, unpaired t test, paired versus unpaired CS+/US; Figures S3F and S5A–S5C), suggesting that LTP in these pathways was not due to nonspecific effect of the US. As ACx and MGN inputs can convey distinct information to the LA and play different roles in discriminative fear conditioning (Antunes and Moita, 2010), we examined these pathways separately and found that the AMPA/NMDA ratio was significantly higher in the FC group than in the NS group in the ACx-LA pathway ($p < 0.05$, unpaired t test; Figures S5D–S5F), but not in the MGN-LA pathway ($p = 0.63$, unpaired t test; Figures S5G and S5H), indicating postsynaptically expressed LTP was selectively induced in the ACx-LA pathway in discriminative fear learning. In the ACx/MGN inputs to the amygdalo-striatal transition area (ASt), we did not detect significant difference in the AMPA/NMDA ratio between groups ($p = 0.35$, unpaired t test; Figures S5I–S5K), suggesting that LTP associated with discriminative fear learning is pathway specific.

To detect changes in synaptic efficacy by presynaptic expression mechanisms, we examined progressive block of NMDAR EPSC by MK-801, which inhibited NMDAR gradually upon repeated photostimulation (Figures S4N and S4O). We compared between groups the decay constant of the NMDAR EPSC, which is inversely related to presynaptic release probability (Hessler et al., 1993; Rosenmund et al., 1993). There was no significant difference in the NMDAR EPSC decay constant

(K) Histogram showing the distribution of the peak amplitude of EPSCs induced and recorded as in (I) and (J). A normal distribution curve is also shown.
(L) Comparisons of EPSC amplitude (mean ± SD, left) and its coefficient of variation (CV, right) between tone-specific and nonspecific ACx/MGN-LA pathways. EPSCs in tone-specific ACx/MGN-LA pathways were recorded as in (A) and (F), whereas EPSCs in nonspecific ACx/MGN-LA synapses were recorded as in (I) and (J).
See also Figure S2.

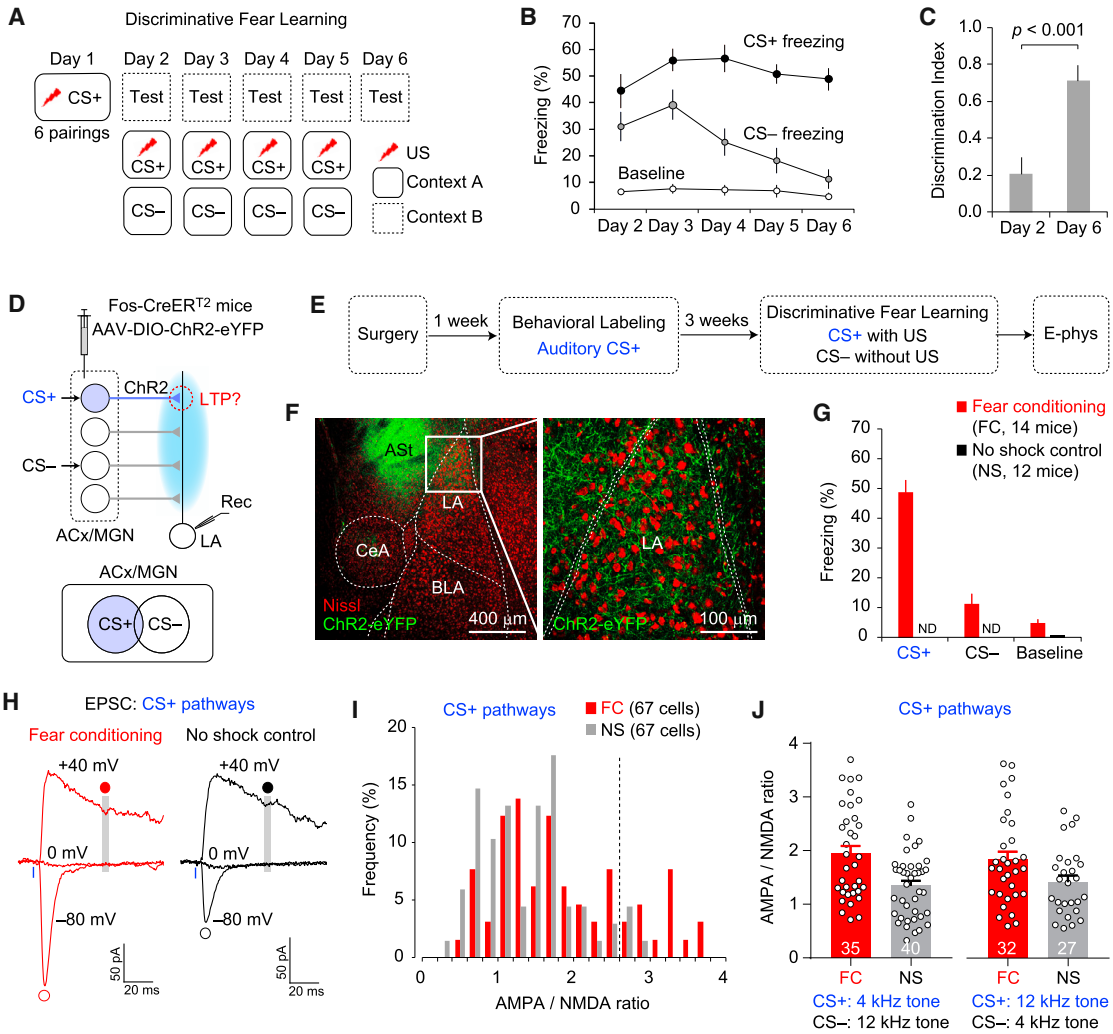

Figure 3. Postsynaptically Expressed LTP Was Induced in the CS+ Pathways to the LA in Auditory Discriminative Fear Conditioning

(A) Auditory discriminative fear conditioning protocol. Two auditory cues (4 and 12 kHz tone, 20 s duration, 70–75 dB) were used as the CS+ and CS– (counterbalanced). On day 1, mice received six pairings of the CS+ and US in context A (Figure S3A). On days 2–5, mice were tested for freezing behavior to the CS+ and CS– in context B (Figure S3B). Mice then received a single pairing of the CS+ and US and were also presented the CS– without the US in context A (Figure S3C).

(B) Quantification of freezing behavior to the CS+ and CS– in discriminative fear conditioning. Baseline immobility was quantified as the percentage of time when the mice were immobile in the absence of the CS+ or CS–.

(C) Plot of the discrimination index before (day 2) and after multiple-trial training (day 6). Fear discrimination index (DI) was calculated using the equation DI = (CS+ freezing − CS− freezing)/(CS+ freezing + CS− freezing). n = 26 mice.

(D) Diagram showing the experimental approach for recording synaptic responses in the CS+ pathways, which convey auditory CS+ information to the LA. After behavioral labeling, ACx/MGN neurons responding to the CS+ expressed ChR2-eYFP. Photostimulation in the amygdala induces postsynaptic responses in the CS+ pathways to the LA.

(E) Experimental setup for (F)–(J). Mice were exposed to the auditory CS+ for behavioral labeling as in Figure 1B. Mice in the fear conditioning (FC) group were trained as in (A). Mice in the no shock (NS) control group received the CS+ and CS– as in the FC group, but the CS+ was not paired with the US.

(F) Microscopic images of the amygdala (left) and LA (right) showing ChR2-eYFP-expressing projections from behaviorally labeled ACx/MGN neurons (green).

(G) Quantification of freezing behavior to the CS+ and CS– in the FC and NS groups on day 6. ND, not detected.

(H) Representative traces of EPSCs recorded in the FC and NS groups. EPSCs were induced by blue light illumination of ChR2-expressing axons and recorded at –80, 0, and +40 mV in voltage-clamp mode in the same LA neurons. AMPAR EPSCs were quantified as the peak amplitude of EPSCs recorded at –80 mV (open circles). NMDAR EPSCs were quantified as the average EPSC amplitude from 47.5 to 52.5 ms after the onset of photostimulation (gray vertical lines and closed circles). SR-95531 (10 μM) was added to block inhibitory postsynaptic currents.

(I) Histogram showing the distribution of the AMPA/NMDA ratio in the FC (red) and NS groups (gray). A dotted vertical line indicates the mean + 2 SDs of the AMPA/NMDA ratio in the NS group.

(J) Comparison of the AMPA/NMDA ratio in the CS+ pathways to the LA between groups. Open circles indicate the AMPA/NMDA ratio calculated in each neuron. Numbers within the bars are the number of neurons examined in each group. Error bars are SEM.

See also Figures S3–S5.

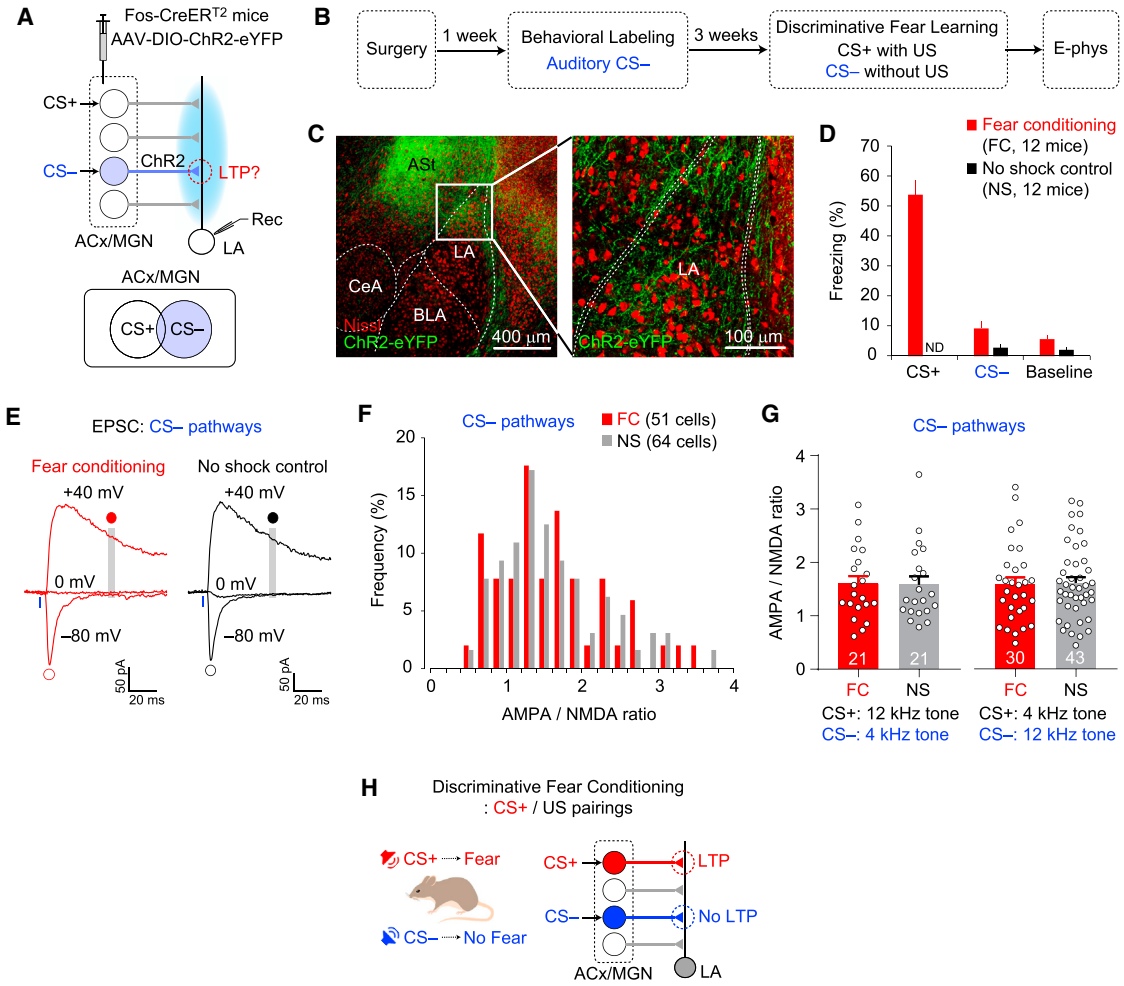

Figure 4. Postsynaptically Expressed LTP Was Not Detected in the CS– Pathways to the LA in Auditory Discriminative Fear Conditioning

(A) Experimental setup for recording synaptic responses in the auditory CS– pathways to the LA. After behavioral labeling, ACx/MGN neurons responding to the CS– (blue) expressed ChR2-eYFP. Photostimulation selectively activated the CS– pathways and induced postsynaptic responses in LA neurons.

(B) Mice were exposed to the auditory CS– (4 or 12 kHz tone, counterbalanced) for behavioral labeling as in Figure 1B. Mice in the fear conditioning (FC) group were trained with the discriminative fear conditioning protocol as in Figure 3A, whereas mice in the no shock (NS) control group received the same CS+ and CS– without the US.

(C) Microscopic images of the amygdala (left) and the LA (right) showing ChR2-eYFP-expressing projections of behaviorally labeled ACx/MGN neurons (green).

(D) Quantification of freezing behavior to the CS+ and CS– in the FC and NS groups on day 6. ND, not detected.

(E) Representative traces of EPSCs recorded in the FC and NS groups. Both AMPAR and NMDAR EPSCs were recorded in each LA neuron, and the AMPA/NMDA EPSC ratio was calculated as in Figure 3H.

(F) Histogram showing the distribution of the AMPA/NMDA ratio in the FC (red) and NS groups (gray).

(G) Comparison of the AMPA/NMDA ratio in the CS– pathways to the LA between groups.

(H) Auditory discriminative fear conditioning induces LTP selectively in the CS+ pathways to the LA, resulting in conditioned fear responses to the CS+, but not to the CS–. Error bars are SEM.

See also Figures S3 and S4.

between groups ($p = 0.11$, unpaired t test; Figure S4P), indicating that discriminative fear learning did not affect presynaptic release probability in the CS+ pathways to the LA.

Postsynaptically Expressed LTP Was Not Detected in the CS– Pathways to the LA in Auditory Discrimination Fear Learning

In discriminative fear learning, mice initially displayed fear to the auditory CS–, which gradually decreased after multiple-trial fear conditioning (Figures 3A–3C). We hypothesized that reduced fear to the CS– was due to the lack of LTP in the pathways conveying CS– information to the LA. We tested this hypothesis by examining how synaptic efficacy changed in the CS– pathways in discriminative fear conditioning (Figure 4A). For behavioral labeling, we exposed mice to the auditory CS– to induce ChR2 expression in ACx/MGN neurons responding to the CS– (Figures 4B and 4C). As in previous experiments, mice in the FC group received the CS+ paired with the US, whereas mice

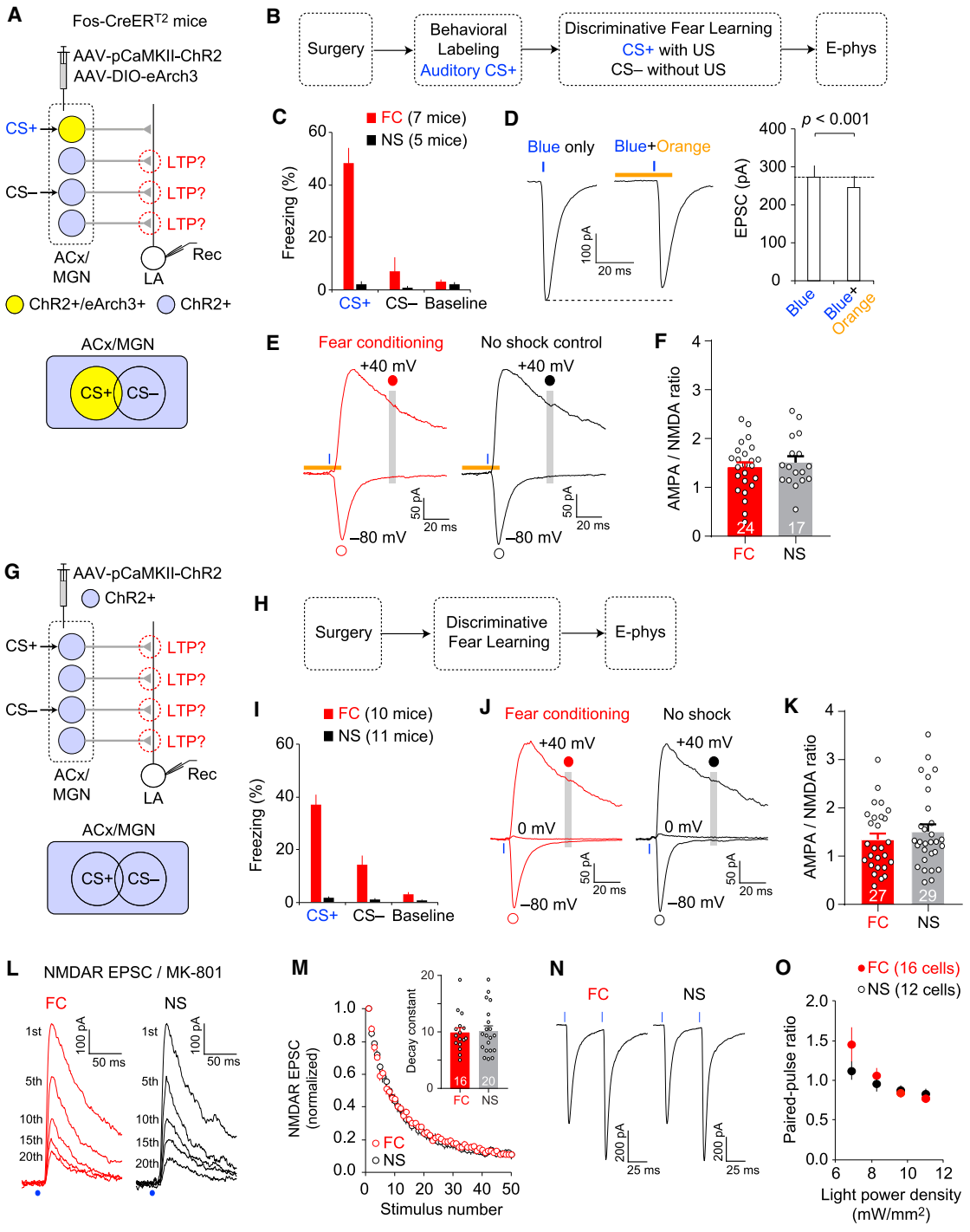

Figure 5. LTP Was Not Induced Globally in the ACx/MGN-LA Pathways in Discriminative Fear Learning

(A) Experimental setup for (B)–(F). ChR2 was expressed globally in ACx and MGN (blue), whereas eArch3 was expressed in CS+-responding ACx/MGN neurons (yellow).

(B) Mice were exposed to the auditory CS+ for behavioral labeling as in Figure 1B. Mice in the fear conditioning (FC) group were trained with the discriminative fear learning protocol as in Figure 3A. Mice in the no shock (NS) group received the same CS+ and CS– without the US.

(C) Quantification of freezing behavior to the CS+ and CS– in the FC and NS groups on day 6.

(D) Left: representative traces of EPSCs induced by blue light illumination (blue vertical bars), which globally activated ACx/MGN inputs to the LA. EPSCs were recorded at –80 mV in LA neurons. The EPSC amplitude was reduced when eArch3-activating orange light (590 nm LED, 30 ms duration, orange horizontal bar) was also applied. Right: quantification of the orange light effect on EPSCs induced by blue light.

(legend continued on next page)

in the NS control group received the CS+ and CS– without the US. After discriminative fear conditioning, mice in the FC group displayed robust freezing behavior to the CS+ but a much lower fear response to the CS– (Figures 4D and S3E). In brain slices, we photostimulated ACx/MGN axons conveying the CS− information and recorded EPSCs in LA neurons (Figures 4A and 4E). In the CS– pathways to the LA, there was no difference in the AMPA/NMDA EPSC ratio between the FC and NS groups (Figures 4E–4G; main effect of groups, $p = 0.95$; main effect of tone frequency, $p = 1.00$; groups × tone frequency interaction, $p = 0.86$; two-way ANOVA). For presynaptically expressed synaptic changes, we compared the rate of progressive block of NMDAR EPSC by MK-801 and found no significant difference in the decay constant between groups ($p = 0.40$, unpaired t test; Figures S4Q–S4S). These results suggest that synaptic efficacy did not change in the CS– pathways to the LA by either presynaptic or postsynaptic mechanisms in discriminative fear learning. We also analyzed the effects of behaviorally labeled auditory pathways (CS+ versus CS– pathways) and behavioral groups (FC versus NS) on the AMPA/NMDA EPSC ratio and found a significant pathways × groups interaction ($p < 0.01$, two-way ANOVA; Figures 3J and 4G; Table S1), indicating that postsynaptically expressed LTP was induced in the CS+ pathways, but not in the CS– pathways to the LA in discriminative fear conditioning (Figure 4H).

LTP Was Not Induced Globally in the ACx/MGN-LA Pathways in Discriminative Fear Learning

In discriminative fear learning, postsynaptically expressed LTP was detected in the auditory CS+, but not CS–, pathways to the LA. We next investigated whether discriminative fear conditioning globally induced LTP in the ACx/MGN-LA pathways by examining synaptic efficacy in randomly selected ACx/MGN-LA synapses while excluding the contribution of the LTP in the CS+ pathways for our assay. To this end, we co-injected AAV-pCaMKIIα-ChR2-eYFP and AAV-pEF1α-DIO-eArch3-eYFP into ACx and MGN in Fos-CreER^{T2} mice. ChR2 was expressed globally in ACx/MGN under the control of the CaMKIIα promoter, whereas eArch3 expression was limited to ACx/MGN neurons responding to the auditory CS+ after behavioral labeling (Figures 5A and 5B). We then trained mice in the FC group for discriminative fear to the CS+ (Figure 5C). Mice in the NS group did not show fear responses to either the CS+ or CS–. In brain slices, we globally activated ACx/MGN inputs to the LA with ChR2-activating blue light while silencing the CS+ pathways with eArch3-activating orange light. Illumination with both blue and orange lights significantly reduced EPSC amplitude by 13.1% ± 2.2% (mean ± SEM, $n = 36$ neurons) compared with that of EPSCs induced by blue light alone ($p < 0.001$, paired t test; Figure 5D). The effect was mediated by eArch3 expressed in a subset of the ACx/MGN-LA pathways (Figures S6A–S6D). Effective silencing of the CS+ pathways was further confirmed in another experiment, in which both ChR2 and eArch3 were expressed selectively in CS+-responding ACx/MGN neurons (Figures S6E–S6G). With this approach, we recorded EPSCs in randomly selected ACx/MGN-LA pathways to the LA, excluding synaptic responses in the CS+-specific synapses. Under this condition, the AMPA/NMDA EPSC ratio was not significantly different between the FC and NS groups ($p = 0.91$, unpaired t test; Figures 5E and 5F), suggesting that postsynaptically expressed LTP was not induced globally in the ACx/MGN-LA pathways in discriminative fear conditioning.

Consistently, we did not detect a significant difference in the AMPA/NMDA EPSC ratio between groups when we globally photostimulated the ACx/MGN-LA pathways, including the CS+ pathways ($p = 0.40$, unpaired t test; Figures 5G–5K). Under this condition, there was no significant difference between groups in the rate of progressive block of NMDAR EPSC by MK-801 ($p = 0.83$, unpaired t test; Figures 5L and 5M) or paired-pulse ratio, which is inversely related to the presynaptic release probability (Zucker and Regehr, 2002) (main effect of groups, $p = 0.48$; groups × intensity interaction, $p = 0.10$, repeated-measures two-way ANOVA; Figures 5N and 5O). These results suggest that LTP by either presynaptic or postsynaptic expression mechanisms was not induced globally in the ACx/MGN-LA pathways. Moreover, we did not detect a significant difference between groups in either the amplitude or frequency of spontaneous EPSCs (sEPSCs), which reflect synaptic responses in nonspecific presynaptic inputs to the LA ($p = 0.34$ and $p = 0.66$ for sEPSC amplitude and frequency, respectively, unpaired t test; Figures S6H–S6L). Taken together, our results suggest that LTP was not induced globally in the ACx/MGN-LA pathways in auditory discriminative fear conditioning.

(E) Representative traces of EPSCs recorded in the FC and NS groups. Both blue and orange light illumination was applied to induce EPSCs in the LA as in (D). AMPAR and NMDAR EPSCs were recorded in the same LA neurons, and the AMPA/NMDA EPSC ratio was calculated as in Figure 3H.
(F) Quantification of the AMPA/NMDA ratio in the FC and NS groups.
(G) Experimental setup for (H)–(O). ChR2 was expressed globally in the ACx and MGN.
(H) Mice in the FC group were trained with the discriminative fear learning protocol, whereas mice in the NS group received the same CS+ and CS– without the US.
(I) Quantification of freezing behavior to the CS+ and CS– in the FC and NS groups on day 6.
(J) Representative traces of EPSCs recorded in LA neurons in the FC and NS groups. EPSCs were induced by blue light alone.
(K) Quantification of the AMPA/NMDA EPSC ratio in the FC and NS groups.
(L) Traces of NMDAR EPSCs evoked by the *n*th photostimulation after MK-801 application (10 μM), showing progressive block of NMDAR EPSCs by MK-801. NMDAR EPSCs were recorded at +40 mV in the presence of NBQX (10 μM) and SR-95531 (10 μM).
(M) Plot showing a gradual decrease of NMDAR EPSCs by MK-801. The peak amplitude of NMDAR EPSCs was normalized to the first NMDAR EPSC induced after MK-801 application for 10–15 min and plotted versus photostimulation number. Inset: quantification of the rate of NMDAR EPSC decrease by MK-801. The decay constant was calculated as in Figure S4P.
(N) Representative traces of EPSCs induced by paired photostimulations (blue vertical bars) with a 50 ms interval in the FC and NS groups.
(O) Comparison of paired-pulse ratio plotted versus photostimulation intensity. Error bars are SEM.
See also Figure S6.

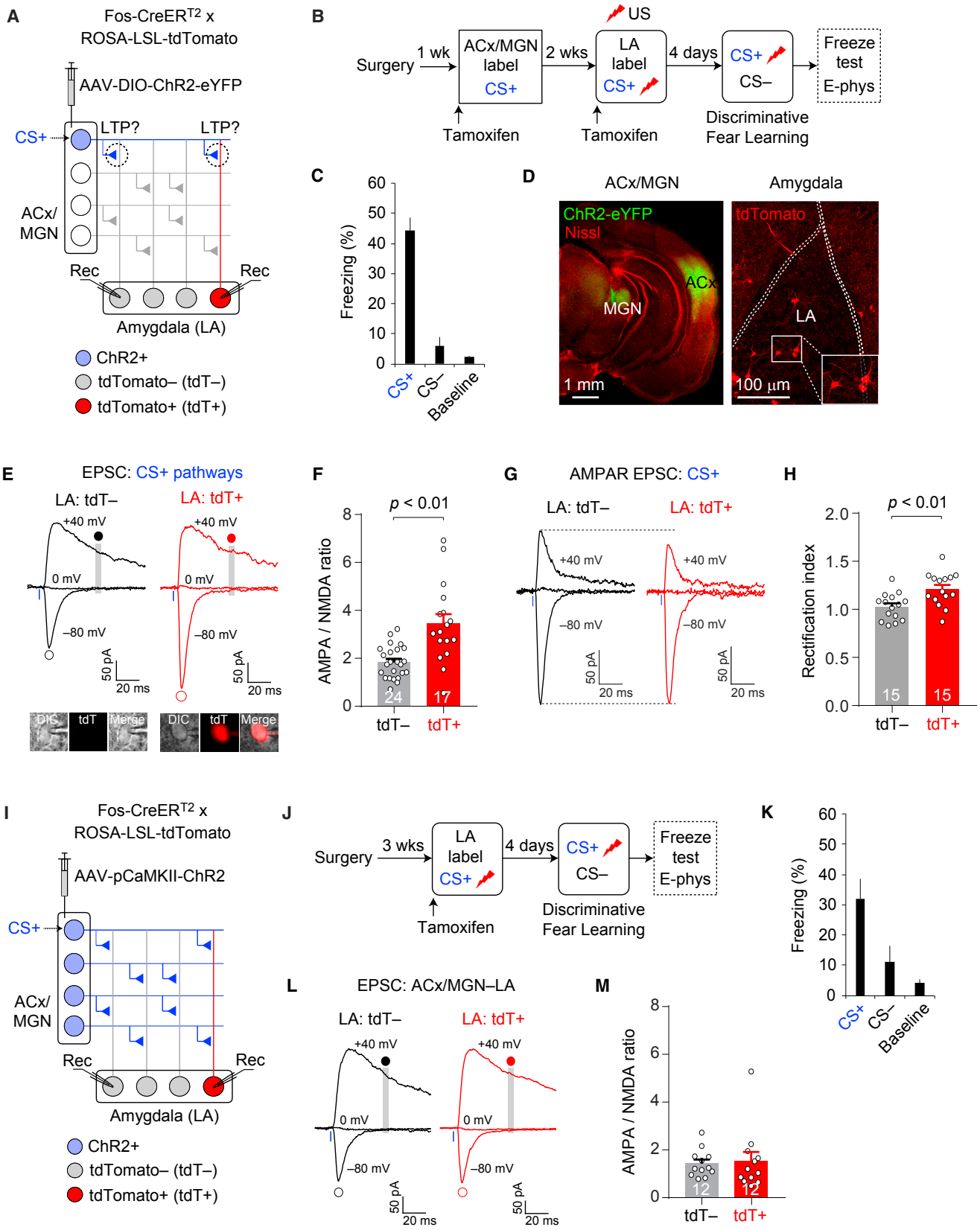

(legend on next page)

LTP Was Preferentially Induced in the Auditory CS+ Inputs to a Subset of LA Neurons Activated during Fear Conditioning

Our results demonstrate that postsynaptically expressed LTP is selectively induced in the inputs conveying CS+ information to the LA in auditory discriminative fear learning (Figures 3, 4, and 5) and the input-specific LTP was detected in only a small population (approximately 20%) of postsynaptic LA neurons (Figure 3I). The activation of presynaptic inputs followed by backpropagating action potentials in postsynaptic neurons with a short time interval induces associative Hebbian plasticity in the ACx/MGN-LA pathways (Humeau et al., 2005; Shin et al., 2006). Thus, LTP may be induced preferentially in synapses consisting of presynaptic ACx/MGN inputs and postsynaptic LA neurons that are activated during the CS/US pairings. To test this possibility, we injected AAV-pEF1α-DIO-ChR2-eYFP into ACx and MGN in Fos-CreER^{T2} × ROSA-LSL-tdTomato mice (Figure 6A). We employed dual behavioral labeling, in which CS+-responding presynaptic ACx/MGN neurons were labeled with ChR2 and postsynaptic LA neurons activated during fear conditioning were labeled with tdTomato (Figures 6A and 6B). After behavioral labeling, mice were trained for discriminative fear responses selectively to the CS+ (12 kHz tone; Figure 6C). In brain slices, LA neurons activated during fear conditioning were identified with tdTomato expression (Figure 6D). We induced EPSCs with photostimulation of CS+-responding ACx/MGN axons and compared EPSCs recorded in tdTomato-labeled and unlabeled LA neurons. The AMPA/NMDA EPSC ratio was significantly higher in tdTomato-labeled neurons than in unlabeled neurons ($p < 0.01$, unpaired t test; Figures 6E and 6F), suggesting that CS+ pathway-specific LTP was preferentially induced in a subset of postsynaptic LA neurons activated during fear conditioning. Moreover, we observed more pronounced inward rectification of AMPAR EPSC in tdTomato+ neurons than in unlabeled LA neurons ($p < 0.01$, unpaired t test; Figures 6G and 6H), suggesting that postsynaptic increase in GluA2-lacking AMPAR contributes to LTP induced preferentially in the fear engram pathways (Clem and Huganir, 2010; Plant et al., 2006; Rumpel et al., 2005). We also found that prior discriminative fear learning occluded additional LTP induced in brain slices in the CS+ pathways to tdTomato+ neurons (Figures S7A–S7F). Together, these results suggest that discriminative fear learning preferentially induced LTP in the CS+ pathways to LA neurons that are activated during fear conditioning.

We next examined whether discriminative fear learning was associated with enhanced synaptic efficacy in the randomly selected ACx/MGN-LA pathways to LA neurons activated during fear conditioning. To this end, we injected AAV-pCaMKIIα-ChR2-eYFP into ACx and MGN in the Fos-CreER^{T2} × ROSA-LSL-tdTomato mice for global ChR2 expression in the auditory areas and labeled LA neurons activated during fear conditioning with tdTomato (Figures 6I and 6J). After discriminative fear conditioning (Figure 6K), we induced EPSCs with photostimulation of randomly selected ACx/MGN inputs and recorded AMPAR and NMDAR EPSCs in LA neurons. There was no significant difference in the AMPA/NMDA ratio between labeled and unlabeled LA neurons ($p = 0.80$, unpaired t test; Figures 6L and 6M), suggesting that synaptic efficacy in randomly selected ACx/MGN inputs was not preferentially altered in LA neurons activated during fear conditioning. We also compared sEPSCs and found no significant difference in the amplitude or frequency of sEPSCs between tdTomato-labeled and unlabeled LA neurons ($p = 0.73$ and $p = 0.21$ for sEPSC amplitude and frequency, respectively, unpaired t test; Figures S7G–S7I). Taken together, our results suggest that discriminative fear learning is associated with LTP, which is preferentially induced in presynaptic ACx/MGN inputs conveying CS+ information to a subset of postsynaptic LA neurons activated during fear conditioning.

Figure 6. LTP Was Induced Preferentially in the Auditory CS+ Inputs to a Subset of LA Neurons Activated during Fear Conditioning

(A) Experimental setup for (B)–(H). LA neurons activated during fear conditioning were labeled with tdTomato. Photostimulation activated axons of CS+-responding ACx/MGN neurons and induced synaptic responses in tdTomato+ or tdTomato– neurons in the LA (Rec).

(B) Mice were exposed to the auditory CS+ for ChR2-eYFP expression in CS+-responding ACx and MGN as in Figure 1B. Mice then received the second tamoxifen injection and were presented with six pairings of the CS+ and US for tdTomato (tdT) expression in LA neurons activated during fear conditioning. After LA labeling, mice were trained with the discriminative fear learning protocol as in Figure 3A.

(C) Quantification of freezing responses to the auditory CS+ and CS– on day 5. n = 10 mice.

(D) Left: microscopic image of coronal brain sections showing ChR2-eYFP-expressing neurons (green) in ACx and MGN. Right: image of the LA showing tdTomato-labeled LA neurons (red).

(E) Representative traces of EPSCs recorded in tdTomato– and tdTomato+ neurons. tdTomato+ neurons were identified with red fluorescence within the LA (inset). EPSCs were induced by photostimulation of ChR2-expressing axons. Both AMPAR and NMDAR EPSCs were recorded in the same LA neurons as in Figure 3H.

(F) Quantification of the AMPA/NMDA ratio in tdTomato– and tdTomato+ LA neurons.

(G) Representative traces of AMPAR-mediated EPSCs recorded in tdTomato– and tdTomato+ neurons. AMPAR EPSCs were induced by photostimulation of ChR2-expressing axons and recorded at –80, 0, and +40 mV in the presence of D-AP5 (50 μM) and SR-95531 (10 μM).

(H) Quantification of the rectification index (RI), which was calculated from the equation $RI = (EPSC_{-80} / 80)/(EPSC_{+40} / 40)$, where $EPSC_{-80}$ and $EPSC_{+40}$ are peak amplitude of EPSCs recorded at –80 and +40 mV, respectively.

(I) Experimental setup for (J)–(M). Photostimulation globally activated the ACx/MGN-LA pathways and induced postsynaptic responses recorded in tdTomato+ or tdTomato– neurons in the LA.

(J) After surgery, mice underwent behavioral labeling of the LA and were trained with the discriminative fear conditioning protocol.

(K) Quantification of freezing responses to the auditory CS+ and CS– on day 5. n = 5 mice.

(L) Representative traces of EPSCs recorded in tdTomato– and tdTomato+ neurons.

(M) Quantification of the AMPA/NMDA ratio in tdTomato– and tdTomato+ LA neurons when the ACx/MGN-LA pathways were photostimulated globally. Error bars are SEM.

See also Figure S7.

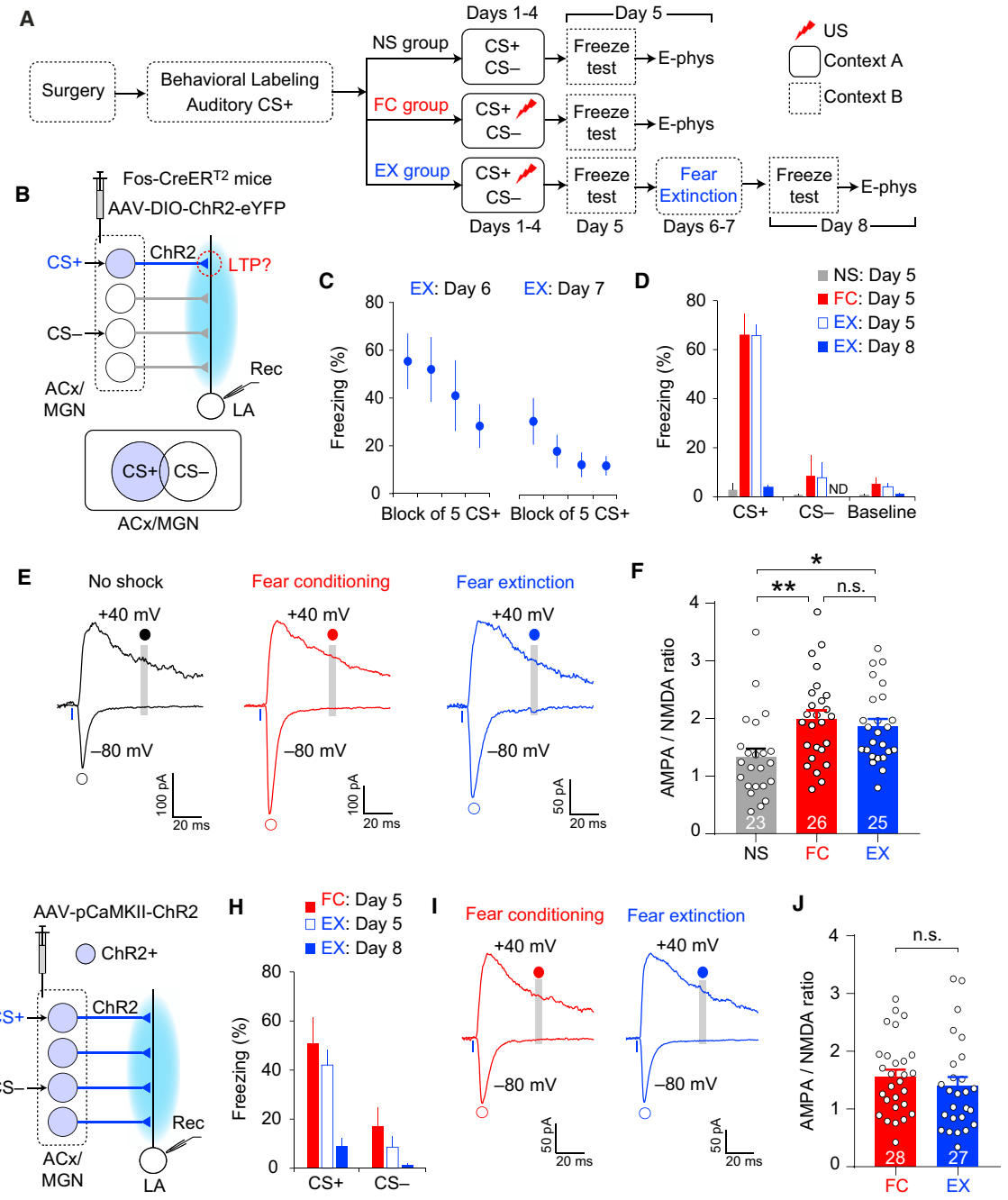

Figure 7. Synapses in the CS+ Pathways to the LA Remained Potentiated after Extinction of Discriminative Fear Memory for the CS+

(A) Experimental setup for behavioral labeling with the auditory CS+ and training mice in no shock (NS), fear conditioning (FC), and fear extinction groups (EX).

(B) Experimental setup for (C)–(F) for recording EPSCs in the CS+ pathways to the LA, which were compared between groups to examine how discriminative fear conditioning and extinction affected synaptic efficacy in these pathways.

(C) Time course of freezing behavior to the CS+ during fear extinction learning on days 6 and 7 in the EX group.

(D) Quantification of freezing behavior to the auditory CS+ and CS– in the NS (5 mice, day 5), FC (6 mice, day 5), and EX groups (5 mice, days 5 and 8). ND, not detected.

(E) Representative traces of EPSCs recorded in LA neurons in the NS, FC, and EX groups. EPSCs were induced by photostimulation of ChR2-expressing ACx/MGN axons in the amygdala. Both AMPAR and NMDAR EPSCs were recorded in the same LA neurons as in Figure 3H.

(F) Quantification of the AMPA/NMDA ratio. *p < 0.05, **p < 0.01; n.s., non-significant.

(G) Experimental setup for (H)–(J). Photostimulation globally activated the ACx/MGN-LA pathways and induced postsynaptic responses, which were compared between the FC and EX groups.

(legend continued on next page)

Synapses in the CS+ Pathways to the LA Remained Potentiated after Extinction of Discriminative Fear Memory for the CS+

Conditioned fear memory can be extinguished by repeated CS presentations without the US. A previous report suggests the presence of fear extinction-associated synaptic changes in the auditory pathways to the LA (Kim et al., 2007). Because the formation of discriminative fear memory involves LTP selectively induced in the neural pathways conveying CS+ information to the LA, we examined how the extinction of discriminative fear memory affected synaptic efficacy in the CS+-specific pathways to the LA. We induced ChR2 expression in ACx/MGN neurons responding to the CS+ by injecting AAV-pEF1α-DIO-ChR2-eYFP into ACx and MGN in Fos-CreER^{T2} mice and exposing them to the auditory CS+ (12 kHz tone) (Figures 7A and 7B). Mice in the FC group received discriminative fear conditioning with the CS+ paired with the US and displayed discriminative fear to the CS+ (Figures 7A and 7D). In the fear extinction group (EX), we induced extinction of the discriminative fear with repeated CS+ presentations after discriminative fear conditioning (Figures 7A and 7C). Fear extinction training for 2 days significantly reduced fear response to the CS+ ($p < 0.01$, day 5 versus day 8, paired t test; Figure 7D). Mice in the NS control group received CS+ and CS– without the US and showed no fear to either the CS+ or CS– (Figures 7A and 7D). In brain slices, we compared between groups EPSCs that were evoked by photostimulation of axons of CS+-responding ACx/MGN neurons and recorded in LA neurons. In CS+ pathways to the LA, the AMPA/NMDA EPSC ratio was significantly different between behavioral groups ($p < 0.01$, one-way ANOVA; Figures 7E and 7F). Post hoc analysis revealed that the AMPA/NMDA ratio was significantly higher in the FC and EX groups than in the NS group ($p < 0.01$, FC versus NS; $p < 0.05$, EX versus NS; Figure 7F), whereas there was no significant difference between the FC and EX groups ($p = 1.00$), suggesting that synaptic efficacy remains enhanced in the auditory CS+ pathways to the LA after the extinction of discriminative fear memory for the CS+. When ChR2 was globally expressed in ACx and MGN (Figures 7G and 7H), the AMPA/NMDA ratio in the EX group was not significantly different from that in the FC group ($p = 0.40$, unpaired t test; Figures 7I and 7J), suggesting that synaptic efficacy in nonspecific ACx/MGN-LA pathways was not altered after fear extinction.

Optogenetically Induced Depotentiation of the CS-Specific ACx/MGN-LA Pathways Prevented the Recall of Fear Memory for the CS

Our results demonstrate that postsynaptically expressed LTP is induced selectively in the ACx/MGN pathways conveying CS+ information to the LA in discriminative fear learning. We next determined whether input-specific LTP is necessary for the conditioned fear response by examining how input-specific depotentiation (the reversal of LTP) in the CS-specific ACx/MGN-LA pathways affected fear responses to the CS. To this end, we induced ChR2 expression in ACx/MGN neurons responding to 4 or 12 kHz tone. In brain slices, we then selectively photostimulated tone-specific ACx/MGN-LA pathways and recorded EPSCs in LA neurons (Figure 8A). After the baseline recording of EPSC, we applied 1 Hz photostimulations for 5 min with a holding potential of –60 mV, which induced a long-lasting reduction of the EPSC in the tone-specific ACx/MGN-LA pathways (53.1% ± 8.4% of baseline, $p < 0.01$, paired t test; Figures 8B and 8C).

We next applied low-frequency photostimulations in vivo to induce depotentiation in the CS-specific ACx/MGN-LA pathways, which had been potentiated after fear conditioning (Figure 8D). We injected AAV-pEF1α-DIO-ChR2-eYFP (ChR2-eYFP group) or AAV-pEF1α-DIO-eYFP (eYFP group) into ACx and MGN in Fos-CreER^{T2} mice (Figure 8E). An optical cannula was implanted dorsal to the ipsilateral LA (Figures 8E, 8F, S8A, and S8B), and NMDA was injected into the contralateral amygdala for an excitotoxic lesion (Figure S8C). After surgery, mice received behavioral labeling with the auditory CS+ (12 kHz tone) for ChR2-eYFP or eYFP expression in ACx/MGN neurons responding to the CS+. Mice were habituated to optical cable connection on days 1–4 and fear conditioned with CS+/US pairings on days 5 and 6 (Figures 8G and S8D), which resulted in freezing behavior to the CS+ on day 7 in both groups (Figure 8H). Mice then received 1 Hz photostimulations for 15 min on days 7–9 (Figures 8G and S8D). After in vivo photostimulations for 3 days, mice in the ChR2-eYFP group displayed significantly reduced freezing behavior to the CS+ ($p < 0.01$, day 7 versus day 10; Figures 8H and S8E), whereas the same photostimulations did not significantly affect fear response to the CS+ in the eYFP control group ($p = 0.53$, Figures 8H and S8E) (groups × photostimulation interaction, $p < 0.05$; repeated-measures two-way ANOVA with post hoc multiple comparisons). These results indicate that reduced fear responses after photostimulation depended on ChR2 expression in CS+-responding ACx/MGN neurons. Moreover, the AMPA/NMDA ratio of EPSCs in the CS+-specific ACx/MGN-LA pathways was significantly reduced in brain slices from mice that received 1 Hz photostimulation after fear conditioning, compared with that of mice that did not receive 1 Hz photostimulation after fear conditioning ($p < 0.05$, unpaired t test; Figures 8K and 8L), indicating that in vivo photostimulation induced depotentiation in the CS-specific ACx/MGN-LA pathways. However, the same 1 Hz photostimulations did not affect the AMPA/NMDA ratio in the CS-specific ACx/MGN-ASt pathways ($p = 0.15$, unpaired t test; Figures S8G and S8H). Taken together, our results suggest that depotentiation in the CS+-specific ACx/MGN-LA pathways was sufficient to prevent fear responses to the CS+. Therefore, LTP in the auditory CS+-specific pathways to the LA is necessary for conditioned fear response to the CS+.

(H) Quantification of freezing behavior to the auditory CS+ and CS– in the FC (5 mice, day 5) and EX groups (5 mice, days 5 and 8).
(I) Representative EPSC traces in the FC and EX groups. EPSCs were induced by photostimulation of randomly selected ACx/MGN inputs to the LA. Both AMPAR and NMDAR EPSCs were recorded in the same LA neurons as in (E).
(J) Quantification of the AMPA/NMDA ratio. Error bars are SEM.

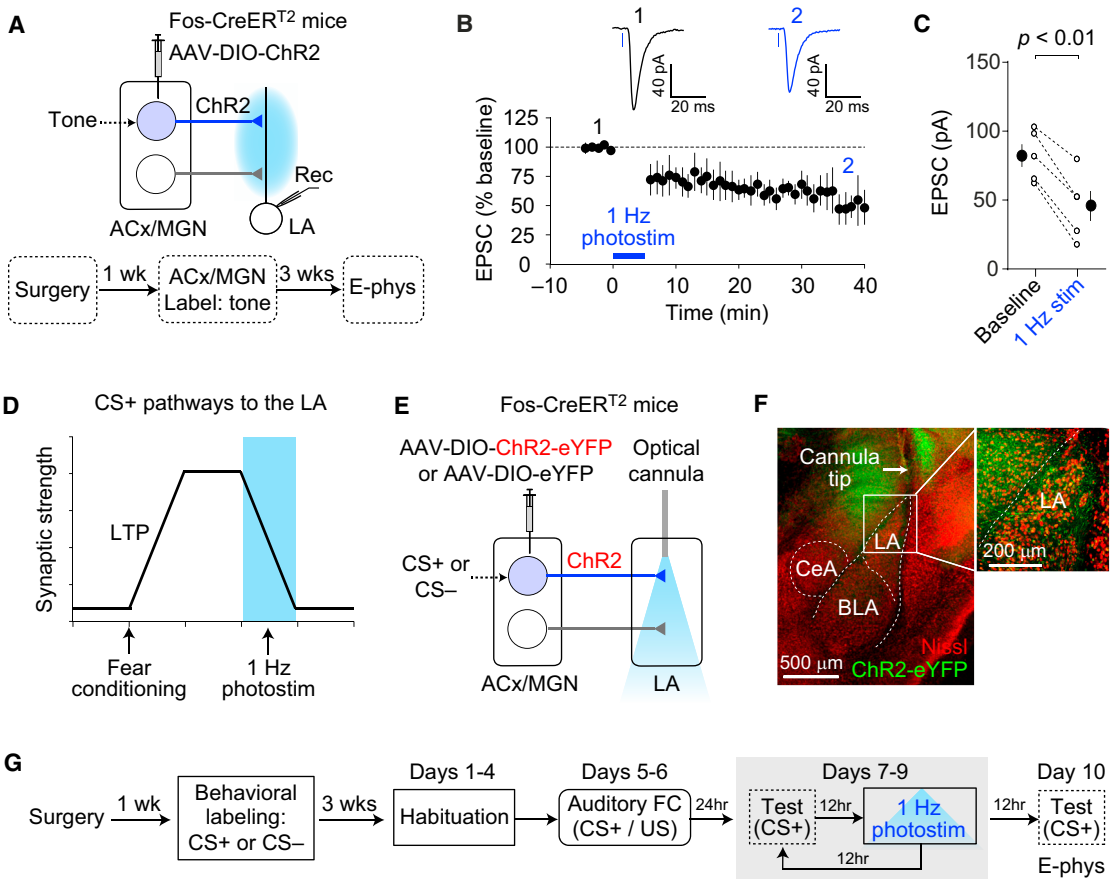

(legend on next page)

We also examined how in vivo photostimulations applied to the CS– pathways to the LA affected conditioned fear responses to the CS+. After surgery (Figures 8E and 8F), we used our behavioral labeling protocol for the expression of ChR2 or eYFP in ACx/MGN neurons responding to the CS– (Figure 8G). Mice were fear conditioned to the CS+ and then received in vivo photostimulations at 1 Hz for 3 days as in previous experiments. Freezing behavior to the CS+ after in vivo photostimulations (day 10) was not significantly different from freezing behavior before photostimulations (day 7) in either the ChR2 or eYFP group (Figures 8I, 8J, and S8F) (main effect of group, $p = 0.23$; main effect of photostimulation, $p = 0.06$; groups × photostimulation interaction, $p = 0.66$; repeated-measures two-way ANOVA). These results indicate that low-frequency photostimulation of the CS– pathways to the LA did not affect conditioned fear response to the CS+. Therefore, observed behavioral effects of photostimulation in the CS+ pathways in our previous experiments are not attributable to the effect of photostimulation in nonspecific input pathways.

DISCUSSION

Our results demonstrate that LTP in the CS-specific ACx/MGN-LA pathways could contribute to encoding discriminative fear memory for the CS. Our neural activity-dependent behavioral labeling approach enabled the recording of synaptic responses in the CS-specific pathways and revealed a population of LA neurons that preferentially receives presynaptic inputs conveying specific auditory information. With this approach, we found that postsynaptically expressed LTP was induced selectively in the pathways conveying auditory CS+ information to the LA, whereas LTP was not detected in either the CS– pathways or randomly selected ACx/MGN-LA synapses in discriminative fear conditioning. Input-specific LTP was induced preferentially in a subset of LA neurons activated during auditory fear conditioning. CS-specific ACx/MGN-LA synapses remained potentiated after fear extinction. Moreover, depotentiation of the CS-specific ACx/MGN-LA pathways prevented the recall of fear memory for the CS, suggesting that input-specific LTP is necessary for conditioned fear responses to a specific auditory cue.

One of the most commonly used approaches to discover the synaptic correlates of an associative memory is to examine learning-induced changes in synaptic strength in relevant circuits with electrophysiological recordings in brain slices from trained animals. In conventional recordings, synaptic responses are induced by electrical stimulations of presynaptic inputs and recorded in postsynaptic neurons (McKernan and Shinnick-Gallagher, 1997). Recent advances in optogenetics enable more selective activations of presynaptic inputs and more accurate recordings of synaptic responses at the neural circuit level (Cho et al., 2013; Li et al., 2013). Even with these approaches, however, it was still challenging to examine synaptic function in functionally defined presynaptic inputs and detect input-specific LTP efficiently with sufficient statistical power. This challenge was overcome in our study with a novel combined approach of behavioral labeling, optogenetic stimulation, and electrophysiological recordings. Neural activity-dependent expression of ChR2 by behavioral labeling enabled selective optogenetic stimulation of the CS-specific pathways in brain slices and the analysis of input-specific synaptic changes in discriminative fear learning, which were previously unattainable through conventional approaches. With our novel approach, we identified a population of LA neurons that receives presynaptic inputs from ACx/MGN neurons responding to a specific auditory stimulus. Our study suggests that heterogeneous populations of LA neurons receive ACx/MGN inputs conveying different auditory CS information while the total number of ACx/MGN inputs to each LA neuron is uniform.

Figure 8. Optogenetically Induced Depotentiation in the CS-Specific ACx/MGN-LA Pathways Prevented the Recall of Fear Memory for the CS

(A) Experimental setup for (B) and (C). Blue light illumination selectively activated axons of tone-responding ACx/MGN neurons and induced EPSCs in LA neurons.

(B) Repeated photostimulation (1 ms pulses) at 1 Hz for 5 min with 10 s pauses every minute induced a lasting reduction of EPSCs in tone-specific ACx/MGN-LA pathways. Top: representative traces of EPSCs recorded at –80 mV in an LA neuron before (1, black) and 30 min after 1 Hz photostimulations (2, blue). Bottom: time course of EPSC changes induced by 1 Hz photostimulations (n = 5 neurons). EPSC amplitude was normalized to the baseline EPSC.

(C) Graph showing significant reduction of EPSC amplitude after 1 Hz photostimulations. EPSCs recorded 30–35 min after 1 Hz photostimulations were averaged and compared with the baseline EPSCs.

(D) Diagram showing changes in synaptic efficacy in the CS+ ACx/MGN-LA pathways after fear conditioning and 1 Hz low-frequency photostimulations.

(E) Diagram showing the experimental approach for in vivo photostimulation of auditory CS+ or CS– pathways to the LA.

(F) Microscopic image of the amygdala and LA showing the eYFP-labeled axons (green) of CS-responding ACx/MGN neurons and the cannula implantation site (arrow).

(G) Experimental setup for (H)–(L). After fear conditioning on days 5 and 6, mice received 1 Hz photostimulations for 15 min through the optical cannula on days 7–9 (Figure S8D). On day 10, mice were tested for freezing behavior to the CS+ and electrophysiological recordings were performed in brain slices.

(H) Left: freezing behavior to the CS+ before and after 3 days of 1 Hz photostimulations of CS+ pathways, which significantly reduced freezing behavior to the CS+ in the ChR2-eYFP group (n = 6 mice). Right: the same photostimulations did not significantly affect freezing behavior to the CS+ in the eYFP group (n = 6 mice). Open circles indicate freezing responses to the CS+ in each mouse on days 7 and 10. Closed circles are the average of freezing responses.

(I) Freezing behavior to the CS+ before and after 3 days of 1 Hz photostimulations of CS– pathways in the ChR2-eYFP group (n = 6 mice, left) and eYFP group (n = 6 mice, right).

(J) Quantification of reduction in freezing behavior to the CS+ (% baseline) after 1 Hz photostimulations of the CS+ or CS– pathways to the LA. Two-way ANOVA (groups × pathways interaction, $p < 0.05$) with post hoc comparisons.

(K) Representative traces of EPSCs recorded in brain slices from mice in the ChR2-eYFP group. Left: EPSCs recorded in an LA neuron in mice that were fear conditioned but did not receive 1 Hz photostimulations in vivo (black, FC/photostim–). Right: EPSCs recorded in an LA neuron in mice that received 1 Hz photostimulations in vivo after fear conditioning (blue, FC/photostim+). AMPAR and NMDAR EPSCs recorded as in Figure 3H.

(L) Quantification of the AMPA/NMDA ratio calculated as in (K). Error bars are SEM.

See also Figure S8.

LTP in the ACx/MGN-LA pathways plays an essential role in the formation of associative fear memory. As the specific auditory CS activates only a subset of ACx/MGN neurons projecting to the amygdala, LTP is thought to be induced selectively in neural pathways conveying the CS signals to the amygdala for encoding associative fear memory, and the input-specific LTP could confer fear memory specificity, enabling adaptive fear responses only to the relevant sensory cue or context. However, it was unknown whether LTP is induced globally or selectively in the CS-specific pathways to the LA in associative fear learning. In previous studies with in vivo recording, discriminative fear conditioning was associated with a more robust potentiation of single-unit activity and local field potential in the LA to the CS+ than to the CS–, suggesting that the responsiveness of the LA was increased selectively to the CS+ (Collins and Paré, 2000; Ghosh and Chattarji, 2015; Goosens et al., 2003). However, prior studies with electrophysiological recordings in brain slices suggest that LTP may be induced globally in the ACx/MGN-LA pathways in auditory fear conditioning. Although synaptic responses in the LA were evoked by electrical stimulations of randomly selected ACx/MGN inputs in these studies, auditory fear conditioning was associated with the robust potentiation of synaptic efficacy in the ACx/MGN-LA pathways (Clem and Huganir, 2010; Kim et al., 2007; McKernan and Shinnick-Gallagher, 1997; Rumpel et al., 2005) and an occlusion of LTP in brain slices (Cho et al., 2011; Tsvetkov et al., 2002). In our current study, we directly examined how synaptic efficacy in the CS+ and CS– pathways to the LA changed after discriminative fear conditioning. Our results suggest that synaptic potentiation with postsynaptic expression mechanisms was induced selectively in the auditory CS+ pathways to the LA, but not the CS– pathways, in discriminative fear conditioning. Notably, LTP with either presynaptic or postsynaptic expression mechanisms was not detected in randomly selected ACx/MGN-LA pathways, indicating that LTP was not induced globally in the ACx/MGN-LA pathways in discriminative fear learning. Our results diverge from previous reports, in which robust LTP was detected in randomly selected ACx/MGN-LA pathways. Differences in fear conditioning protocols may account for the discrepancy. We employed multiple-trial fear conditioning for discriminative fear conditioning, whereas previous studies used single-trial fear conditioning, in which fear memory could have been non-discriminative, and LTP may have been induced globally in non-discriminative fear learning.

We also identified a subset of LA neurons in which input-specific LTP was preferentially induced in discriminative fear learning. The activation of presynaptic inputs followed by back-propagating action potentials in postsynaptic neurons with a short time interval induces associative Hebbian plasticity in the ACx/MGN-LA pathways (Humeau et al., 2005; Shin et al., 2006). In auditory fear conditioning, the CS-US pairings activate only a subset of ACx/MGN and LA neurons. Thus, LTP may be induced preferentially in synapses consisting of presynaptic ACx/MGN and postsynaptic LA neurons that are activated during the CS-US pairings. To test this possibility, we labeled postsynaptic LA neurons that are activated during fear conditioning and recorded in these neurons synaptic responses evoked by selective stimulation of the CS+-specific ACx/MGN inputs. After discriminative fear conditioning, both the AMPA/NMDA EPSC ratio and rectification index of AMPAR EPSC were higher in labeled LA neurons than in randomly selected unlabeled LA neurons, suggesting that input-specific LTP was preferentially induced in a subset of the ACx/MGN-LA synapses that are activated during fear conditioning. Previous studies have utilized approaches to capture and permanently tag neuronal ensembles in the amygdala that are active during fear memory encoding (Reijmers et al., 2007; Tayler et al., 2013) (for review, see Josselyn et al., 2015). Our results are consistent with previous reports that a subset of LA neurons are recruited preferentially into a fear memory trace (Han et al., 2007) and undergo LTP associated with fear conditioning (Gouty-Colomer et al., 2016; Nonaka et al., 2014). These LA neurons may receive more robust presynaptic inputs conveying the CS and/or US information or have higher neuronal excitability, which facilitates LTP induction during the CS-US pairings (Gouty-Colomer et al., 2016; Yiu et al., 2014).

We also found that CS-specific ACx/MGN-LA synapses remained potentiated even after the extinction of discriminative fear memory. There has been controversy in previous studies regarding the synaptic mechanisms of fear extinction. Some studies suggest that fear extinction is associated with the depotentiation of the MGN-LA pathway (Kim et al., 2007). In other studies, the MGN-LA pathway remained potentiated after fear extinction (Clem and Huganir, 2010), and optogenetically induced LTP in the ACx/MGN-LA pathways did not reverse fear extinction (Nabavi et al., 2014), suggesting that fear extinction learning does not involve depotentiation in the ACx/MGN-LA pathways. Unlike previous studies in which synaptic responses were analyzed in randomly selected ACx/MGN-LA synapses, we examined the CS-specific ACx/MGN-LA pathways in fear extinction because discriminative fear learning involves LTP selectively induced in the CS-specific pathways to the LA. We found that these pathways remained potentiated after fear extinction, which supports the theoretical models of extinction that posit inhibitory regulation of extant plasticity rather than the erasure of LTP. Fear extinction is new learning leading to the formation of extinction memory, which suppresses the expression of conditioned fear (Herry et al., 2010; Maren, 2011). If fear extinction induces depotentiation of the ACx/MGN-LA pathways, in which fear memory is encoded, it should irreversibly erase the fear memory. After fear extinction, however, conditioned fear can recover spontaneously with the mere passage of time or recur after contextual changes or the exposure to a stressful event, suggesting the original fear memory is not erased after fear extinction (Herry et al., 2010; Maren, 2011). Thus, depotentiation does not fully account for the recurrence of fear memory after fear extinction. Our results suggest that fear extinction learning does not require depotentiation of the ACx/MGN-LA pathways but may involve synaptic plasticity in other neural circuits, including the mPFC-amygdala pathways (Bukalo et al., 2015; Cho et al., 2013; Do-Monte et al., 2015).

Our study implicates the input-specific LTP in encoding fear memory for the specific auditory cue. A previous study demonstrated that optogenetically induced LTD in the ACx/MGN-LA pathways prevented conditioned fear responses to the auditory cue (Nabavi et al., 2014), suggesting that LTP in these pathways is necessary for auditory fear conditioning. As their optogenetic

stimulations globally induced LTD in nonselective ACx/MGN-LA pathways, it remained to be determined whether the formation of specific fear memory requires global or input-specific LTP. With our behavioral labeling and in vivo optogenetic approaches, we could selectively stimulate the CS+ or CS– ACx/MGN-LA pathways and modulate synaptic efficacy in vivo in an input-specific manner. Low-frequency stimulations of the CS+, but not CS–, pathways to the LA prevented conditioned fear responses to the CS+. As our behavioral labeling induced transgene expression in only 10%–15% of ACx/MGN neurons projecting to the LA, our results suggest that depotentiation of a small but CS+-specific population of the ACx/MGN-LA pathways was sufficient to prevent fear responses to the CS+, indicating that the formation of discriminative fear memory requires input-specific LTP in the ACx/MGN-LA pathways. Our findings also provide important insights for the development of a novel approach to attenuate pathological fear in post-traumatic stress disorder and specific phobias because depotentiation that reverses the input-specific LTP could suppress maladaptive fear without affecting adaptive fear memories, enhancing therapeutic tolerance.

STAR★METHODS

Detailed methods are provided in the online version of this paper and include the following:

- KEY RESOURCES TABLE
- CONTACT FOR REAGENT AND RESOURCE SHARING
- EXPERIMENTAL MODEL AND SUBJECT DETAILS
- METHOD DETAILS
  - Virus Constructs
  - Surgery
  - Behavioral Labeling
  - Auditory Discriminative Fear Conditioning
  - In vivo Optogenetic Stimulation
  - Histology and Microscopic Imaging
  - Cell Counting
  - Whole-Cell Patch-Clamp Recording in Brain Slices
- QUANTIFICATION AND STATISTICAL ANALYSIS

SUPPLEMENTAL INFORMATION

Supplemental Information includes eight figures and three tables and can be found with this article online at http://dx.doi.org/10.1016/j.neuron.2017.08.004.

A video abstract is available at http://dx.doi.org/10.1016/j.neuron.2017.08.004#mmc3.

AUTHOR CONTRIBUTIONS

Conceptualization, J.-H.C.; Methodology, J.-H.C.; Formal Analysis, J.-H.C.; Investigation, W.B.K. and J.-H.C.; Writing – Original Draft, J.-H.C.; Writing – Review & Editing, W.B.K. and J.-H.C.; Visualization, J.-H.C.; Supervision, J.-H.C.; Funding Acquisition, J.-H.C.

ACKNOWLEDGMENTS

We thank Dr. Edward Korzus and Dr. Ben Huang for experimental advice and Dr. Rachael Neve for HSV packaging. This study was supported by the Initial Complement Funds from the University of California, Riverside (J.-H.C.).

Received: February 28, 2017
Revised: July 9, 2017
Accepted: August 1, 2017
Published: August 17, 2017

REFERENCES

Antunes, R., and Moita, M.A. (2010). Discriminative auditory fear learning requires both tuned and nontuned auditory pathways to the amygdala. J. Neurosci. *30*, 9782–9787.

Bukalo, O., Pinard, C.R., Silverstein, S., Brehm, C., Hartley, N.D., Whittle, N., Colacicco, G., Busch, E., Patel, S., Singewald, N., and Holmes, A. (2015). Prefrontal inputs to the amygdala instruct fear extinction memory formation. Sci. Adv. *1*, e1500251.

Cho, J.H., Bayazitov, I.T., Meloni, E.G., Myers, K.M., Carlezon, W.A., Jr., Zakharenko, S.S., and Bolshakov, V.Y. (2011). Coactivation of thalamic and cortical pathways induces input timing-dependent plasticity in amygdala. Nat. Neurosci. *15*, 113–122.

Cho, J.H., Deisseroth, K., and Bolshakov, V.Y. (2013). Synaptic encoding of fear extinction in mPFC-amygdala circuits. Neuron *80*, 1491–1507.

Clem, R.L., and Huganir, R.L. (2010). Calcium-permeable AMPA receptor dynamics mediate fear memory erasure. Science *330*, 1108–1112.

Collins, D.R., and Paré, D. (2000). Differential fear conditioning induces reciprocal changes in the sensory responses of lateral amygdala neurons to the CS(+) and CS(-). Learn. Mem. *7*, 97–103.

Do-Monte, F.H., Manzano-Nieves, G., Quiñones-Laracuente, K., Ramos-Medina, L., and Quirk, G.J. (2015). Revisiting the role of infralimbic cortex in fear extinction with optogenetics. J. Neurosci. *35*, 3607–3615.

Ghosh, S., and Chattarji, S. (2015). Neuronal encoding of the switch from specific to generalized fear. Nat. Neurosci. *18*, 112–120.

Goosens, K.A., Hobin, J.A., and Maren, S. (2003). Auditory-evoked spike firing in the lateral amygdala and Pavlovian fear conditioning: mnemonic code or fear bias? Neuron *40*, 1013–1022.

Gouty-Colomer, L.A., Hosseini, B., Marcelo, I.M., Schreiber, J., Slump, D.E., Yamaguchi, S., Houweling, A.R., Jaarsma, D., Elgersma, Y., and Kushner, S.A. (2016). Arc expression identifies the lateral amygdala fear memory trace. Mol. Psychiatry *21*, 1153.

Gründemann, J., and Lüthi, A. (2015). Ensemble coding in amygdala circuits for associative learning. Curr. Opin. Neurobiol. *35*, 200–206.

Guenthner, C.J., Miyamichi, K., Yang, H.H., Heller, H.C., and Luo, L. (2013). Permanent genetic access to transiently active neurons via TRAP: targeted recombination in active populations. Neuron *78*, 773–784.

Han, J.H., Kushner, S.A., Yiu, A.P., Cole, C.J., Matynia, A., Brown, R.A., Neve, R.L., Guzowski, J.F., Silva, A.J., and Josselyn, S.A. (2007). Neuronal competition and selection during memory formation. Science *316*, 457–460.

Herry, C., Ferraguti, F., Singewald, N., Letzkus, J.J., Ehrlich, I., and Lüthi, A. (2010). Neuronal circuits of fear extinction. Eur. J. Neurosci. *31*, 599–612.

Hessler, N.A., Shirke, A.M., and Malinow, R. (1993). The probability of transmitter release at a mammalian central synapse. Nature *366*, 569–572.

Humeau, Y., Herry, C., Kemp, N., Shaban, H., Fourcaudot, E., Bissière, S., and Lüthi, A. (2005). Dendritic spine heterogeneity determines afferent-specific Hebbian plasticity in the amygdala. Neuron *45*, 119–131.

Josselyn, S.A., Köhler, S., and Frankland, P.W. (2015). Finding the engram. Nat. Rev. Neurosci. *16*, 521–534.

Kauer, J.A., Malenka, R.C., and Nicoll, R.A. (1988). A persistent postsynaptic modification mediates long-term potentiation in the hippocampus. Neuron *1*, 911–917.

Kim, J., Lee, S., Park, K., Hong, I., Song, B., Son, G., Park, H., Kim, W.R., Park, E., Choe, H.K., et al. (2007). Amygdala depotentiation and fear extinction. Proc. Natl. Acad. Sci. USA *104*, 20955–20960.

LeDoux, J.E. (2000). Emotion circuits in the brain. Annu. Rev. Neurosci. *23*, 155–184.

Li, H., Penzo, M.A., Taniguchi, H., Kopec, C.D., Huang, Z.J., and Li, B. (2013). Experience-dependent modification of a central amygdala fear circuit. Nat. Neurosci. *16*, 332–339.

Maren, S. (2001). Neurobiology of Pavlovian fear conditioning. Annu. Rev. Neurosci. *24*, 897–931.

Maren, S. (2011). Seeking a spotless mind: extinction, deconsolidation, and erasure of fear memory. Neuron *70*, 830–845.

McKernan, M.G., and Shinnick-Gallagher, P. (1997). Fear conditioning induces a lasting potentiation of synaptic currents in vitro. Nature *390*, 607–611.

Muller, D., Joly, M., and Lynch, G. (1988). Contributions of quisqualate and NMDA receptors to the induction and expression of LTP. Science *242*, 1694–1697.

Nabavi, S., Fox, R., Proulx, C.D., Lin, J.Y., Tsien, R.Y., and Malinow, R. (2014). Engineering a memory with LTD and LTP. Nature *511*, 348–352.

Nonaka, A., Toyoda, T., Miura, Y., Hitora-Imamura, N., Naka, M., Eguchi, M., Yamaguchi, S., Ikegaya, Y., Matsuki, N., and Nomura, H. (2014). Synaptic plasticity associated with a memory engram in the basolateral amygdala. J. Neurosci. *34*, 9305–9309.

Plant, K., Pelkey, K.A., Bortolotto, Z.A., Morita, D., Terashima, A., McBain, C.J., Collingridge, G.L., and Isaac, J.T. (2006). Transient incorporation of native GluR2-lacking AMPA receptors during hippocampal long-term potentiation. Nat. Neurosci. *9*, 602–604.

Reijmers, L.G., Perkins, B.L., Matsuo, N., and Mayford, M. (2007). Localization of a stable neural correlate of associative memory. Science *317*, 1230–1233.

Rogan, M.T., Stäubli, U.V., and LeDoux, J.E. (1997). Fear conditioning induces associative long-term potentiation in the amygdala. Nature *390*, 604–607.

Rosenmund, C., Clements, J.D., and Westbrook, G.L. (1993). Nonuniform probability of glutamate release at a hippocampal synapse. Science *262*, 754–757.

Rumpel, S., LeDoux, J., Zador, A., and Malinow, R. (2005). Postsynaptic receptor trafficking underlying a form of associative learning. Science *308*, 83–88.

Shin, R.M., Tsvetkov, E., and Bolshakov, V.Y. (2006). Spatiotemporal asymmetry of associative synaptic plasticity in fear conditioning pathways. Neuron *52*, 883–896.

Tayler, K.K., Tanaka, K.Z., Reijmers, L.G., and Wiltgen, B.J. (2013). Reactivation of neural ensembles during the retrieval of recent and remote memory. Curr. Biol. *23*, 99–106.

Tovote, P., Fadok, J.P., and Lüthi, A. (2015). Neuronal circuits for fear and anxiety. Nat. Rev. Neurosci. *16*, 317–331.

Tovote, P., Esposito, M.S., Botta, P., Chaudun, F., Fadok, J.P., Markovic, M., Wolff, S.B., Ramakrishnan, C., Fenno, L., Deisseroth, K., et al. (2016). Midbrain circuits for defensive behaviour. Nature *534*, 206–212.

Tsvetkov, E., Carlezon, W.A., Benes, F.M., Kandel, E.R., and Bolshakov, V.Y. (2002). Fear conditioning occludes LTP-induced presynaptic enhancement of synaptic transmission in the cortical pathway to the lateral amygdala. Neuron *34*, 289–300.

Yiu, A.P., Mercaldo, V., Yan, C., Richards, B., Rashid, A.J., Hsiang, H.L., Pressey, J., Mahadevan, V., Tran, M.M., Kushner, S.A., et al. (2014). Neurons are recruited to a memory trace based on relative neuronal excitability immediately before training. Neuron *83*, 722–735.

Yizhar, O., Fenno, L.E., Davidson, T.J., Mogri, M., and Deisseroth, K. (2011). Optogenetics in neural systems. Neuron *71*, 9–34.

Zucker, R.S., and Regehr, W.G. (2002). Short-term synaptic plasticity. Annu. Rev. Physiol. *64*, 355–405.

STAR★METHODS

KEY RESOURCES TABLE

REAGENT or RESOURCE	SOURCE	IDENTIFIER
Chemicals, Peptides, and Recombinant Proteins		
AAV-pEF1α-DIO-eYFP	UNC Vector Core	N/A
AAV-pEF1α-DIO-mCherry	UNC Vector Core	N/A
AAV-pEF1α-DIO-ChR2(H143R)-eYFP	UNC Vector Core	N/A
AAV-pCaMKIIα-ChR2(H143R)-eYFP	UNC Vector Core	N/A
AAV-pEF1α-DIO-eArch3-eYFP	UNC Vector Core	N/A
AAV-pSyn-FLEX-ChrimsonR-tdTomato	UNC Vector Core	N/A
HSV-pEF1α-mCherry	MIT Vector Core	N/A
NBQX disodium salt	Tocris Bioscience	Cat# 1044
MK-801	Tocris Bioscience	Cat# 924
D-AP5	Tocris Bioscience	Cat# 0106
SR-95531	Sigma-Aldrich	Cat# S106
Spermine tetrahydrochloride	Tocris Bioscience	Cat# 0958
Biocytin	Tocris Bioscience	Cat# 3349
NMDA	Sigma-Aldrich	Cat# M3262
Tamoxifen	Sigma-Aldrich	Cat# T5648
Corn oil	Sigma-Aldrich	Cat# C8267
Streptavidin-Alexa 568 conjugate	Thermo Fisher	Cat# S11226
Neurotrace 530/615 red fluorescent Nissl stain	Thermo Fisher	Cat# N21482
Vectashield mounting media with DAPI	Vector Laboratories	Cat# H-1200
Experimental Models: Organisms/Strains		
C57BL/6J mice	Jackson Laboratory	Stock # 000664; RRID: IMSR_JAX:000664
Fos-CreERT2 (+/−) mice	Jackson Laboratory	Stock # 021882; RRID: IMSR_JAX:021882
Fos-shGFP (+/−) mice	Jackson Laboratory	Stock # 018306; RRID: IMSR_JAX:018306
Ai9 ROSA-LSL-tdTomato (+/+) mice	Jackson Laboratory	Stock # 007905; RRID: IMSR_JAX:007905
GAD2-IRES-Cre (+/+) mice	Jackson Laboratory	Stock # 010802; RRID: IMSR_JAX:010802
Fos-CreERT2 (+/−) x Fos-shGFP (+/−) mice	This paper	N/A
Fos-CreERT2 (+/−) x ROSA-LSL-tdTomato (+/−) mice	This paper	N/A
Software and Algorithms		
Ethovision XT 11	Noldus	N/A
ImageJ	NIH	N/A
Clampex 10	Molecular Devices	N/A
Clampfit 10	Molecular Devices	N/A
Minitab 17	Minitab	N/A
Prism 7	GraphPad Software	N/A
Other		
Optical cannula (NA 0.53, 200 μm)	Doric Lenses	MFC_200/245-0.53_5mm_MF2.5_FLT
Optical patch cable (NA 0.53)	Doric Lenses	MFP_200/220/900-0.53_0.25m_FC-F2.5
Fiber-optic rotary joints 1x1	Doric Lenses	FRJ_1x1_FC-FC
450 nm Blue laser	Opto Engine	MDL-III-450-200mW
Blue LED	Thorlabs	M470L3
Orange LED	Thorlabs	M590L3
Red LED	Thorlabs	M617L3
LED driver	Thorlabs	LEDD1B

CONTACT FOR REAGENT AND RESOURCE SHARING

Further information and requests for reagents may be directed to and will be fulfilled by the Lead Contact, Jun-Hyeong Cho (juncho@ucr.edu). All published reagents can be shared on an unrestricted basis.

EXPERIMENTAL MODEL AND SUBJECT DETAILS

We obtained heterozygous Fos-CreER^{T2} mice used in this study by crossing wild-type C57BL/6J x Fos-CreER^{T2} (+/−) mice. Fos-CreER^{T2} (+/−) and Fos-shGFP (+/−) mice were crossed to generate Fos-CreER^{T2} (+/−) x Fos-shGFP (+/−) mice. Fos-CreER^{T2} (+/−) and Ai9 ROSA-LSL-tdTomato (+/+) mice were crossed to generate Fos-CreER^{T2} (+/−) x ROSA-LSL-tdTomato (+/−) mice. Mice were singly housed in home cages on a 12-h light/dark cycle with food and water continuously available. The light cycle was from 8 AM to 8 PM. Five- to seven-week-old mice of either sex underwent stereotaxic brain surgery. All of the animal procedures were approved by the Institutional Animal Care and Use Committee of the University of California, Riverside.

METHOD DETAILS

Virus Constructs

The recombinant adeno-associated viruses (AAVs, serotype 5) were packaged by the Vector Core at the University of North Carolina. The AAV titer was 5.6 × 10^{12} genome copies (GC)/mL for AAV-pEF1α-DIO-eYFP, 4.8 × 10^{12} GC/mL for AAV-pEF1α-DIO-mCherry, 4.4-6.6 × 10^{12} GC/mL for AAV-pEF1α-DIO-ChR2(H143R)-eYFP, 8.5 × 10^{12} GC/mL for AAV-pCaMKIIα-ChR2(H143R)-eYFP, 4.4 × 10^{12} GC/mL for AAV-pEF1α-DIO-eArch3-eYFP, and 5.7 × 10^{12} GC/mL for AAV-pSyn-FLEX-ChrimsonR-tdTomato. Herpes simplex viruses (HSV-pEF1α-mCherry) for the retrograde tracing experiments were packaged by Dr. Rachael Neve at the Viral Gene Transfer Core Facility of the Massachusetts Institute of Technology, and the titer was > 3.5 × 10^{9} infectious units/mL.

Surgery

Virus injection surgery

Five- to seven-week-old mice were used for stereotaxic surgery. Prior to surgery, general anesthesia was induced by placing the mice in a transparent anesthetic chamber filled with 5% isoflurane with intramuscular injection of ketamine and xylazine (30 mg/kg and 2 mg/kg body weight, respectively). The anesthesia was maintained during surgery with 1% isoflurane applied to the nostrils of the mice using a precision vaporizer. Mice were checked for the absence of the tail-pinch reflex as a sign of sufficient anesthesia. The mice were then immobilized in a stereotaxic frame with non-rupture ear bars (David Kopf Instruments), and ophthalmic ointment was applied to prevent eye drying. After making an incision to the midline of the scalp, small unilateral or bilateral craniotomies were performed using a microdrill with 0.5-mm burrs. The tips of glass capillaries loaded with AAV were placed into the ACx (2.8 mm caudal to bregma, 4.5 mm lateral to the midline, and 2.5 mm ventral to bregma) and MGN (3.3 mm caudal to bregma, 2.0 mm lateral to the midline, and 3.2 mm ventral to bregma). AAV-containing solution was injected at a rate of 0.1 μL/minute using a 10 μL Hamilton microsyringe and a syringe pump. The total volume of injected virus-containing solution was 0.15 μL for AAV-pCaMKIIα-ChR2(H143R)-eYFP, 0.5 μL for AAV-pEF1α-DIO-ChR2(H143R)-eYFP, 0.5 μL for AAV-pEF1α-DIO-eYFP, 0.85 μL for AAV-pEF1α-DIO-eArch3-eYFP, and 1.0 μL for AAV-pEF1α-DIO-mCherry and AAV-pSyn-FLEX-ChrimsonR-tdTomato. After injection, the capillary was left in place for an additional 5 min to allow for diffusion of the virus solution and then withdrawn. For retrograde tracing in Figures 1F–1H, we injected HSV-pEF1α-mCherry (1.0 μL) to the LA (1.6 mm caudal to bregma, 3.5 mm lateral to the midline, and 4.8 mm ventral to bregma). The scalp incision was closed with surgical suture, and mice were given buprenorphine-containing saline (1 mL, 0.13 mg buprenorphine/kg body weight, subcutaneous injection) for postoperative analgesia and hydration.

Optical cannula implantation and NMDA-induced excitotoxic lesion

For the optogenetically induced depotentiation in Figures 8D–8L, an optical cannula (200 μm in diameter, numeric aperture of 0.53, Doric Lenses) was implanted above the dorsal tip of the left LA (1.7 mm caudal to bregma, 3.7 mm lateral to the midline, and 2.5 mm ventral from the pial surface) and secured with dental cement. To induce an excitotoxic lesion of the right amygdala, *N*-methyl-D-aspartate (NMDA, 0.15 μL, 20 mg/mL) was injected into the right amygdala (1.6 mm caudal to bregma, 3.5 mm lateral to the midline, and 4.8 mm ventral to bregma). We verified the cannula implantation site and NMDA-induced excitotoxic lesion of the amygdala in each animal (Figures S8A–S8C).

Behavioral Labeling

One week after surgery, mice received an intraperitoneal injection of tamoxifen (150-200 mg/kg of body weight, Sigma-Aldrich). Tamoxifen was dissolved in corn oil (Sigma-Aldrich) at 20 mg/mL with nutation for 6 hr in the dark at room temperature (22-24°C). To minimize neuronal labeling by background noise, mice were kept in their home cage in a quiet place with minimal traffic within a satellite animal care facility for 36 hr after tamoxifen injection. Twenty-four hours after tamoxifen injection, the mice were placed in context C (acrylic floor and wall, white light illumination, and no olfactory cue) within a standard fear conditioning chamber (Med Associates) and exposed to pure tone (4 kHz or 12 kHz, 70-75 dB, 5 s duration with 15 s intervals) for 30 min

(Figures 1B and S1A). To reduce context-dependent latent inhibition, mice were kept in context C during behavioral labeling, which is different from the contexts for fear conditioning (context A) and freeze test (context B).

Auditory Discriminative Fear Conditioning

After behavioral labeling, mice were randomly assigned to either the fear conditioning (FC) group or no shock (NS) control group. On the training day (Day 1), mice in the FC group received 6 pairings of the auditory CS+ (70-75 dB pure tone, 20 s duration) and US (electric footshock, 0.5 mA, 2 s duration overlapping with the last 2 s of CS+) with a time interval of 120 s in context A (stainless steel grid floor, white light illumination, and benzaldehyde odor) between 9 AM and 11 AM (Figures 3A and S3A). On Days 2-5, mice were tested for freezing behavior in response to the CS+ and CS− once per day between 9 AM and 11 AM in context B (acrylic plate floor, no illumination, and acetic acid odor) (Figures 3A and S3B). 4 kHz and 12 kHz pure tones were used as the auditory CS+ and CS− (counterbalanced). For testing, mice received two presentations of both CS+ and CS−, and freezing scores were averaged for the CS+ and CS− for each day. Between 6 PM and 8 PM on the same days (Days 2-5), mice received a single pairing of the CS+ and US in context A and then received only CS− without the US in the same context one hour later (Figures 3A and S3C). On Day 6, mice were tested for freezing behavior in response to the CS+ and CS− in context B, and brain slices were prepared from these mice for electrophysiological recording experiments. Mice in the NS control group received the same CS+ and CS− on Days 1-6 as in the FC group but never received the US. Conditioned fear responses to the CS+ and CS− were quantified as % of time immobile to total time of CS+ or CS− presentation. Fear discrimination index (DI) was calculated using the equation, DI = (CS+ freezing − CS− freezing) / (CS+ freezing + CS− freezing) (Figure 3C). The movement of the mice in the fear conditioning chamber was recorded using a near-infrared camera and analyzed in real-time with Ethovision XT 11 software (Noldus). The freezing score was calculated as the percentage of time for which the mice remained immobile. Immobility for more than 2 s during CS+ and CS− presentations was counted as freezing behavior. Baseline immobility was also quantified as the percentage of time when the mice were immobile in the absence of the CS+ or CS– and included in most graphs showing freezing behavior data. The temperature in the fear conditioning chamber was 22-24°C.

For fear conditioning in Figures S5A–S5C, mice in the paired group received a pairing of the CS+ (12 kHz tone, 70-75 dB tone, 20 s duration) and US (0.5 mA electric footshock, 2 s duration overlapping with the last 2 s of CS+) in context A, whereas mice in the unpaired group received the US 300 s after the CS+ presentation (see a diagram in Figure S3F).

For fear extinction training in Figure 7, mice received discriminative fear conditioning on Days 1-4 and then received 20 CS+ presentations with 50 s intervals in context B once per day for 2 days (Days 6-7). On Day 8, mice were tested for freezing behavior to both CS+ and CS− in context B, and brain slices were prepared from these mice for electrophysiological recording experiments.

In vivo Optogenetic Stimulation

For in vivo optogenetic experiments (Figures 8D–8L), AAV-pEF1α-DIO-ChR2-eYFP (ChR2-eYFP group) or AAV-pEF1α-DIO-eYFP (eYFP control group) was injected into ACx and MGN in Fos-CreER^{T2} mice. An optical cannula was implanted targeting the left LA for in vivo optogenetic stimulations, and NMDA was injected into the right amygdala for excitotoxic lesion. One week after surgery, we used our behavioral labeling protocol to induce ChR2 or eYFP expression in ACx/MGN neurons responding to the CS+ (12 kHz tone, 70-75 dB) or CS− (4 kHz tone, 70-75 dB) in context C after tamoxifen administration (Figures 8G and S8D). Three weeks after behavioral labeling, mice were habituated with the optical cannula connected to the optical patch cable without laser stimulation for 10 min once per day for 4 days (Days 1-4) in context C. On the training days (Days 5-6), mice were placed in context A in a fear conditioning chamber without optical cannula connection and given 6 pairings of the auditory CS+ (12 kHz tone, 70-75 dB, 20 s duration) and US (electric footshock, 0.5 mA, 2 s duration overlapping with the last 2 s of CS+) with 120 s time intervals. On the test days (Days 7-10), mice were placed in context B and tested for freezing behavior to the CS+ between 9 AM and 10 AM. After a 2- to 3 min acclimatization period, the CS+ was presented only once per day to minimize fear extinction. Mice displaying robust freezing behavior in response to the CS+ (> 20% freezing time) on Day 7 were included in the in vivo optogenetic experiments. On the same days (Days 7-9), mice were placed in context C with the optical cannula connected to the optical patch cable (200 μm in diameter, numeric aperture of 0.53, Doric lenses) for photostimulations between 7 PM and 8 PM. After a 2 min acclimatization period, mice received 1 Hz pulses of photostimulations (1 ms duration) for 15 min with a 10 s pause every minute once per day (Figure S8D). Blue light illumination was delivered from a blue laser (450 nm, Opto Engine) to the optical cannula through the optical patch cable and optical rotary joint, and the light power was 22-25 mW at the cannula tip. After blue light illumination, mice were left in context C for an additional 3 min. After the final behavioral test on Day 10, brain slices from these mice were prepared for electrophysiological recordings and histological analysis. We verified cannula implantation sites as well as the NMDA-induced excitotoxic lesion of the amygdala in each mouse and excluded mice from analysis when the optical cannula implantation missed the LA.

Histology and Microscopic Imaging

Acute brain slices (300 μm thick) were prepared with a vibratome (VT-1000S, Leica Biosystems) and fixed in 4% paraformaldehyde-containing phosphate buffered saline (PBS, 137 mM NaCl, 2.7 mM KCl, 11.9 mM phosphate, pH 7.4) at 4°C overnight. After fixation, slices were washed twice in PBS containing 0.3% Triton X-100 (PBS-T) at room temperature for 10 min and permeabilized in PBS-T at 4°C overnight. For Nissl staining, slices were incubated with Neurotrace fluorescent Nissl stain (1:40 diluted in PBS, 615 nm emission maximum, Thermo Fisher Scientific) for 3 hr at room temperature and washed in PBS-T three times for 10 min each. After a final

wash in PBS-T, Vectashield mounting media (Vector Laboratories) was applied to the slices, which were then covered with coverslips. Microscopic images were captured using the Leica TCS SP5 confocal system (Leica Microsystems). Images captured with different fluorescent channels were merged using ImageJ software (National Institute of Mental Health). For each mouse, a virus injection site was verified with ChR2-eYFP expression in ACx and MGN. Mice in which the target area was missed were excluded from the analysis. For fluorescent labeling of the recorded neurons (Figure 2E), neurons were loaded with the pipette solution containing 5 mM biocytin for 20 min. The pipette was then withdrawn slowly, and the brain slices were fixed at 4°C overnight with 4% paraformaldehyde. After fixation, slices were washed with PBS-T twice for 10 min each and incubated with streptavidin-Alexa 568 conjugate (20 μg/mL in PBS, Thermo Fisher Scientific) for 2 hr at room temperature. The unbound streptavidin was then washed out with PBS three times for 20 min each, and the slices were mounted onto slides. Images of the labeled neurons were taken using a Leica TSC SP5 confocal microscope, and neuronal morphology and location within the LA were analyzed.

Cell Counting

To quantify the proportion of behaviorally labeled ACx/MGN neurons (eYFP+) among all LA-projecting ACx/MGN neurons (mCherry+) in Figures 1F–1H, confocal microscopic images of 3-4 representative fields (0.56 mm^2) were taken for each mouse with a 20X objective lens using the Leica TCS SP5 confocal system within the ACx and MGN, where mCherry+ neurons were distributed most densely in these areas. The confocal images were then Z stacked using ImageJ software. LA-projecting neurons (mCherry+) and behaviorally labeled neurons (eYFP+) were identified based on the florescence labeling of cell bodies. The proportions of behaviorally labeled ACx/MGN neurons (eYFP+) among all LA-projecting ACx/MGN neurons (mCherry+) were calculated in each field of the ACx/MGN and averaged for each mouse.

To examine the specificity of behavioral labeling in Figures 1I–1K and S1D–S1F, we labeled ACx and MGN neurons at two different time points so that mCherry+ neurons reflected neurons labeled in the remote past, whereas shGFP+ neurons reflected neurons labeled more recently. We captured confocal microscopic images of 3-4 representative fields (0.56 mm^2) with a 20X objective lens in the ACx and MGN, where shGFP-labeled neurons were most abundant within the ACx and MGN. The proportion of shGFP+ neurons among all mCherry+ neurons within the field of view was calculated and averaged for each mouse.

Whole-Cell Patch-Clamp Recording in Brain Slices

For electrophysiological recordings in brain slices, the mice were deeply anesthetized with 5% isoflurane and decapitated. Brains were dissected quickly and chilled in ice-cold artificial cerebrospinal fluid (ACSF) containing 130 mM NaCl, 2.5 mM KCl, 2.5 mM $CaCl_2$, 1 mM $MgSO_4$, 1.25 mM NaH_2PO_4, 26 mM $NaHCO_3$, and 10 mM glucose with 95% O_2 and 5% CO_2. Coronal brain slices containing the amygdala (300-μm thick) were prepared with a vibratome. After a 1 hr recovery period, slices were placed in the recording chamber and continuously perfused with the ACSF at the rate of 1 mL per minute. The patch electrodes (2-3 MΩ resistance) were filled with pipette solution containing 140 mM Cs-methanesulfonate, 5 mM NaCl, 1 mM $MgCl_2$, 10 mM HEPES, 0.2 EGTA, 2 mM MgATP, 0.5 mM NaGTP, and 5 mM QX 314 chloride (290 mOsm, adjusted to pH 7.3 with CsOH). For experiments in Figures 6G and 6H, we added 0.5 mM spermine to the pipette solution. For experiments in Figures S7D–S7F, we replaced 140 mM Cs-methanesulfonate with 150 mM K-gluconate without QX 314 added. We recorded EPSCs in putative principal neurons in the LA with a membrane capacitance larger than 70 pF (see Figures S4A–S4D). For the morphological analysis of recorded neurons in Figure 2E, we added biocytin (5 mM) to the pipette solution. Whole-cell patch clamp recordings were performed at 30-32°C using a Multiclamp 700B amplifier, a Digidata 1550A or 1320A digitizer and Clampex 10 software (Molecular Devices). The membrane potential was held constant at –80 mV in voltage-clamp mode unless otherwise indicated. The liquid junction potential of 8.9 mV was corrected. Series (access) resistance was not compensated. Offline data analysis was performed using the Clampfit 10 program (Molecular Devices). Reagents were prepared as stock solutions in water at 1000-fold concentrations and stored at –20°C.

Photostimulation in brain slices

A blue collimated light-emitting diode (LED) with a peak wavelength of 470 nm (M470L3, Thorlabs) was used for photostimulation of ChR2-expressing axons. The LED was connected to the amplifier and digitizer through the LED driver (LEDD1B, Thorlabs). Brain slices in the recording chamber were illuminated through a 40X water-immersion objective lens (Olympus LUMPLFLN 40XW or Leica HCX APO L40x #506155) and a 450-490 nm filter (Chroma). The illumination area was 0.17 mm^2 and was centered at the soma of the neuron patched for recording. Intensity and duration of photostimulation were controlled using a Digidata 1550A or 1320A digitizer and pClamp 10 software (Molecular Devices). Light power in miliwatts (mW) was measured at 470 nm using a power meter (PM100A, Thorlabs) placed under the objective lens, and light power density (mW/mm^2) was calculated by dividing light power by illumination area. To evoke synaptic responses in the LA by photostimulation of ACx/MGN axons, slices were illuminated every 20 s with blue light pulses of 1 ms duration (light power density: 2.8-20 mW/mm^2 at 470 nm). When apparent polysynaptic activities were detected in EPSC recordings, we reduced photostimulation intensity to prevent the contribution from polysynaptic components to our measurement of AMPAR and NMDAR EPSC amplitudes. When we could not eliminate polysynaptic activities by adjusting the stimulation intensity, we terminated the experiments for the recorded neurons. For the activation of Chrimson-expressing axons (Figures S2H–S2K), an LED with a peak wavelength of 617 nm (M617L3, Thorlabs) was used (55 mW/mm^2 at 617 nm). For the

optogenetic silencing of eArch3-expressing ACx/MGN axons (Figures 5A–5F and S6A–S6G), an LED with a peak wavelength of 590 nm (M590L3, Thorlabs) was used for continuous orange light illumination (12.0 mW/mm^2 at 590 nm), and was turned on 20 ms before and turned off 9 ms after blue light pulses.

AMPA/NMDA EPSC ratio

AMPAR EPSCs were recorded at −80 mV, and NMDAR EPSCs were recorded at +40 mV in voltage-clamp mode. SR-95531 (10 μM), a GABA-A receptor antagonist, was added to the ACSF to prevent the contamination of inhibitory postsynaptic currents in the feed-forward inhibitory circuit. Photostimulation intensity was adjusted such that the peak amplitude of AMPAR EPSC was 50-250 pA. For each LA neuron, the same photostimulation intensity and duration were used to record AMPAR and NMDAR EPSCs. To calculate the AMPA/NMDA EPSC ratio, we recorded the first set of AMPAR EPSCs (3-5 traces) at −80 mV and then recorded NMDAR EPSCs (3-5 traces) at +40 mV. Then, the holding potential was returned to −80 mV to record the second set of AMPAR EPSCs (3-5 traces). We also recorded EPSCs at 0 mV. This recording protocol minimized the effect of time-dependent EPSC changes on the AMPA/NMDA ratio. To quantify AMPAR EPSCs, we averaged AMPAR EPSC traces recorded before and after recording NMDAR EPSCs and calculated the peak amplitude of averaged AMPAR EPSCs. To quantify NMDAR EPSCs, we averaged NMDAR EPSC traces and measured the mean amplitudes of the averaged NMDAR EPSCs between 47.5 ms and 52.5 ms after the onset of photostimulations. Then, we calculated the amplitude ratio of AMPAR EPSCs to NMDAR EPSCs. For each mouse, we typically obtained 2-3 brain slices (300 μm thick) with well-defined LA and recorded AMPAR and NMDAR EPSCs in 2-3 LA neurons per slice.

Progressive block of NMDAR EPSC by MK-801

To compare presynaptic release probability in the ACx/MGN inputs to the LA between behavioral groups, we recorded NMDAR EPSCs at +40 mV in voltage-clamp mode in the presence of NBQX (10 μM) and SR-95531 (10 μM). Photostimulation intensity was adjusted so that the peak amplitude of NMDAR EPSC was 200-500 pA. After baseline recording, the brain slice was perfused with the ACSF containing MK-801 (10 μM) for 10-15 min. Then, we recorded NMDAR EPSCs evoked by photostimulations applied every 10 s. To quantify the rate of NMDAR EPSC decay by MK-801, decay constant (τ) in stimulus number was calculated in each LA neuron by fitting the curve of NMDAR EPSC decrease to a single-exponential equation, $I(n) = I_1\, exp(-n/\tau)$, where n is stimulus number, $I(n)$ is the peak amplitude of nth NMDAR EPSC, and I_1 is the peak amplitude of the first NDMAR EPSC recorded in the presence of MK-801.

Paired-pulse ratio

To calculate the paired-pulse ratio (PPR), AMPAR EPSCs were evoked by paired photostimulations (50 ms interval, 0.5 ms duration) of ChR2-expressing presynaptic axons and recorded in LA neurons at −80 mV in voltage-clamp mode. PPR was calculated as the peak amplitude ratio of the first to the second EPSC. As the PPR was affected by photostimulation intensity, we induced EPSCs with photostimulations of different light intensities and calculated the PPR for each photostimulation intensity in each LA neuron.

Rectification index of AMPAR EPSC

AMPA receptor-mediated EPSCs were induced by photostimulation of ChR2-expressing axons and recorded at –80 and +40 mV in voltage-clamp mode in the presence of D-AP5 (50 μM) and SR-95531 (10 μM). We recorded the first set of AMPAR EPSCs at −80 mV (3-5 traces) and then recorded AMPAR EPSCs at +40 mV (3-5 traces). Then, the holding potential was returned to −80 mV to record the second set of AMPAR EPSCs at −80 mV (3-5 traces). We also recorded EPSCs at 0 mV. To quantify AMPAR EPSCs at –80 mV, we averaged AMPAR EPSC traces recorded at –80 mV before and after recording AMPAR EPSCs at +40 mV and calculated the peak amplitude of averaged AMPAR EPSCs. This recording protocol minimized the effect of time-dependent EPSC changes on the rectification index (RI), which was calculated from the equation, $RI = (EPSC_{-80} / 80) / (EPSC_{+40} / 40)$, where $EPSC_{-80}$ and $EPSC_{+40}$ are peak amplitude of EPSCs recorded at –80 and +40 mV, respectively. The pipette solution contained 0.5 mM spermine, which mediates inward rectification of GluA2-lacking AMPA receptors.

Spontaneous EPSC

Spontaneous EPSCs (sEPSC) were recorded in principal neurons in the LA at −80 mV in voltage-clamp mode for 3-5 min (Figures S6H–S6L and S7G–S7I). The amplitude, inter-event interval and frequency of sEPSC were analyzed using the event detection function of the Clampfit software (Molecular Devices). The average amplitude and frequency of sEPSC were calculated in each LA neuron and were compared between behavioral groups.

QUANTIFICATION AND STATISTICAL ANALYSIS

Data are presented as means ± the standard error of the mean (SEM) unless indicated otherwise. For statistical comparisons, we used Welch's t test (two-tailed), ordinary or repeated-measures ANOVA. For post hoc analysis, we used Bonferroni's simultaneous multiple comparisons. Statistical analysis was performed with Minitab 17 (Minitab) and Prism 7 (GraphPad) software, and $p < 0.05$ was considered statistically significant. Details of statistical analyses are summarized in Tables S1 and S2. Statistical comparisons of passive membrane properties of recorded neurons between groups are summarized in Table S3.